Journal of Earth and Atmospheric Research

PREDICTABILITY OF TOPOGRAPHIC DEVELOPMENTS AND SEDIMENT ACCOMMODATION ACROSS DEEPWATER UPPER SLOPE SUCCESSIONS, OFFSHORE WESTERN NIGER DELTA

[1]Olafiranye, K*, [1]Opeloye, S. A. [1]Amigun, J. O. and [1,2] Adeoye, O. M.

[1]Department of Applied Geology, Federal University of Technology, Akure, Nigeria.
[2]Department of Geology, Federal University Oye-Ekiti, Nigeria.

Article History
Received: 19-04-24
Accepted: 23-08-24

Keywords:
Topographic controls, slope accommodation, grade, sediment gravity flow

ABSTRACT

Biostratigraphic well markers and seismic data were employed to unravel the interplay of depositional processes and topographic controls to account for occurrence of reservoirs resulting from Sediment Gravity Flows (SGF) in the upper slope of deepwater offshore in the western Niger Delta. Wells X and Y as well as 3D seismic reflection data volume covering 300 km2 in water depth of 500 m were used for the studies. Various foraminifera palaeomarkers that mark the tops and bases of identified biozones in well Y were tied to the seismic data for identification of mappable horizon and were also used to age-date the identified seismic units. Across the depositional successions, eleven (11) seismic units were delineated: Five (5) biostratigraphically constrained lower units as well as storeys of six (6) channelized upper units. At the base of each identified units, several occurrences of SGFs were found to have formed in compartments of mini-basins in the Miocene-Pliocene sediments when the depositional regime is out-of-grade. Their formation is related to diapiric process of undercompacted shales while channel developments arose from the healing phase of underlying mini-basins giving rise to graded relief. Given the presence of out-of-grade and graded depositional profiles, the identified systematic coupling has implications for the development of topography and accommodation across the studied successions. The biostratigraphically-constrained aspects of the results provide extended relationship for predicting the depositional processes and products associated with sediment gravity flows in adjoining areas of the study.

Correspondence: kehinde.olafiranye@outlook.com

1 INTRODUCTION

Sediment dispersal and slope grade processes in shelf and slope environments

A typical deepwater sedimentation cycle commences with the activation of shelf-edge repositories during a relative sea-level fall which is marked by a reduction in accommodation on the shelf and an increased supply of sediment to the deepwater environment (Posamentier and Kolla 2003; van der Merwe *et al*., 2010; Tian, *et al.,* 2023; Daniels *et al*., 2024). The cycle concludes with the gradual deactivation of the shelf-edge staging areas during a relative sea-level rise, allowing renewed accommodation on the shelf to trap a significant portion of terrigenous sediment within fluvial to shallow-water systems.

Modifications in the available space on the continental shelf and the positioning of the coastline play a crucial role in governing both the quantity and the grain size of sediment carried by rivers to the deepwater setting (Catuneanu *et al*., 2011). Additionally, the climate and tectonic activity in the source region can influence sediment supply by impacting the size and energy of the rivers responsible for transporting sediment to the coastline. The width of the continental shelf also plays a significant role in this process. 3D volume of seismic data serves as a valuable solution to the challenges associated with observing deepwater processes and products in contemporary environments (Posamentier and Walker, 2006; Weimer and Slatt, 2007). Many of the depositional features forming in deepwater settings are not visible on kilometre-scale, making it difficult for traditional outcrop-based studies to match or surpass the insights provided by high-resolution 3D seismic data. Moreover, today's deep-water environments are often inaccessible, further emphasizing the uniqueness of seismic data as a tool for comprehending deepwater settings, unlike other depositional environments.

After dislodgment from the continental shelf edge, the distance of sediment gravity flows, their deposition locations, and the specific mechanisms and types of these flows are primarily governed by two significant intra-basinal factors - the sea floor gradient and the level of confinement (Pirmez *et al*., 2000). The sea floor gradient, or slope grade, is chiefly controlled by the slope angle and it results in various accommodation types on the slope (Prather *et al*., 1998; Prather, 2000, 2020). This gradient varies along a stratigraphic sequence, transitioning between two extremes: the graded slope and the above-grade slope. A graded slope lacks prominent topographical features, whereas an above-grade slope exhibits well-defined enclosed intra-slope basins or subtle changes in depositional gradient, leading to low-relief stepped or terraced topography.

Distinguishing between above-grade and graded slope types depends on the accommodation type, its extent, and the relationship between a depositional surface and an idealized graded profile. In summary, on an above-grade slope, the delivery and distribution of sediment gravity flows are not very efficient because they tend to concentrate coarser, sandy sediments predominantly around the upslope edge of local topographic highs (Mutti, 1985; Bouma, 2004; Sprague *et al*., 2005; Bauer *et al.,* 2020). However, when these topographic highs are no longer present, the deposition patterns shift to graded slopes, which may reduce the potential for triggering mass movements (Galloway, 1989). During this stage of deposition, sediment is transported through slope bypass and is unconfined and over time, slope instability may develop due to slope oversteepening (Prather *et al*., 1998; Prather, 2000, 2020). The combined outcome of the various slope-building and slope-destroying processes leads to a transformation from an initial theoretical graded profile at a deeper stratigraphic level to a fresh theoretical graded profile at a shallower stratigraphic level. This transformation occurs through the adjustment of both pre-existing and concurrent topographical features (Olafiranye *et al.,* 2013).

Geological setting of Niger Delta

The Niger Delta continental margin, located in the

Gulf of Guinea off the coast of southern Nigeria, stands as one of the world's largest deltaic systems, as documented by Doust and Omatsola (1990). Its terrestrial section spans an area of approximately 75,000 square kilometres and stretches over 300 kilometres from its starting point to its mouth. The regressive delta and the adjoining margin consist of a wedge of clastic sediments, reaching thicknesses of up to 12 kilometres, formed through a series of offlap cycles, as described by Evamy *et al*. (1978) and further elaborated by Doust and Omatsola (1990). The onshore segment of the Niger Delta Province is demarcated by the geological characteristics of southern Nigeria and southwestern Cameroun, as detailed by Tuttle *et al*. (1999). The northern demarcation is established by the Benin flank, an southwest-northeast oriented hinge line situated to the south of the West Africa basement massif. Moving towards the northeastern boundary, it is defined by the Cretaceous Abakaliki High strata and further extends east-southeast to encompass the Calabar flank, a hinge line positioned close to the adjacent Precambrian Basement Complex. The offshore limits of the province are outlined by the Cameroun volcanic line to the east and the eastern section of the Benin (Dahomey) Basin, which represents the easternmost portion of the West African transform-fault passive margin, to the west. To the south and southwest, its boundary is marked by 2000-meter sediment thickness or the 4000-meter bathymetric contour in areas where sediment exceeds 2000 meters in thickness. This province encompasses an area of 300,000 square kilometres and includes the geological expanse of the Tertiary Niger Delta (Akata-Agbada) petroleum system.

This region began undergoing rifting during the Late Jurassic and continued into the Middle Cretaceous (Lehner and De Ruiter, 1977). In the Niger Delta area, the process of rifting gradually diminished and eventually came to a halt in the Late Cretaceous. Following the rifting phase, the primary deformational process shifted to gravity-induced tectonism. The internal deformation of shale resulted from two contributing factors, as noted by Kulke (1995). The first factor was the loading of under-compacted and over-pressured clays found in the prodelta and delta-slope areas of the Akata Formation by higher-density sands located in the delta-front Agbada Formation. The second factor was the onset of slope instability due to the lack of lateral and basinward support for the under-compacted Akata clays on the delta slope. In each deposition belt, gravity tectonics occurred before the deposition of the Benin Formation. This tectonic activity gave rise to intricate geological structures, including shale diapirs, roll-over anticlines, growth faults with collapsed crests, back-to-back fault systems, and steeply dipping, closely spaced flank faults (Evamy *et al*., 1978; Xiao and Suppe, 1992). Damuth (1994) categorized the delta into three primary gravity tectonic regions: (1) the upper extensional zone characterised by listric growth faults situated beneath the outer shelf, (2) the translational zone containing diapirs and shale ridges beneath the upper slope, and (3) the lower compressional zone featuring imbricate thrust structures, also known as toe-thrusts, under the lower slope and rise. Deformation is an ongoing process within these structural zones, leading to noticeable changes in bathymetry that reveal structures unaffected by recent sediment deposition. The inner and outer fold and thrust belts are most prominently

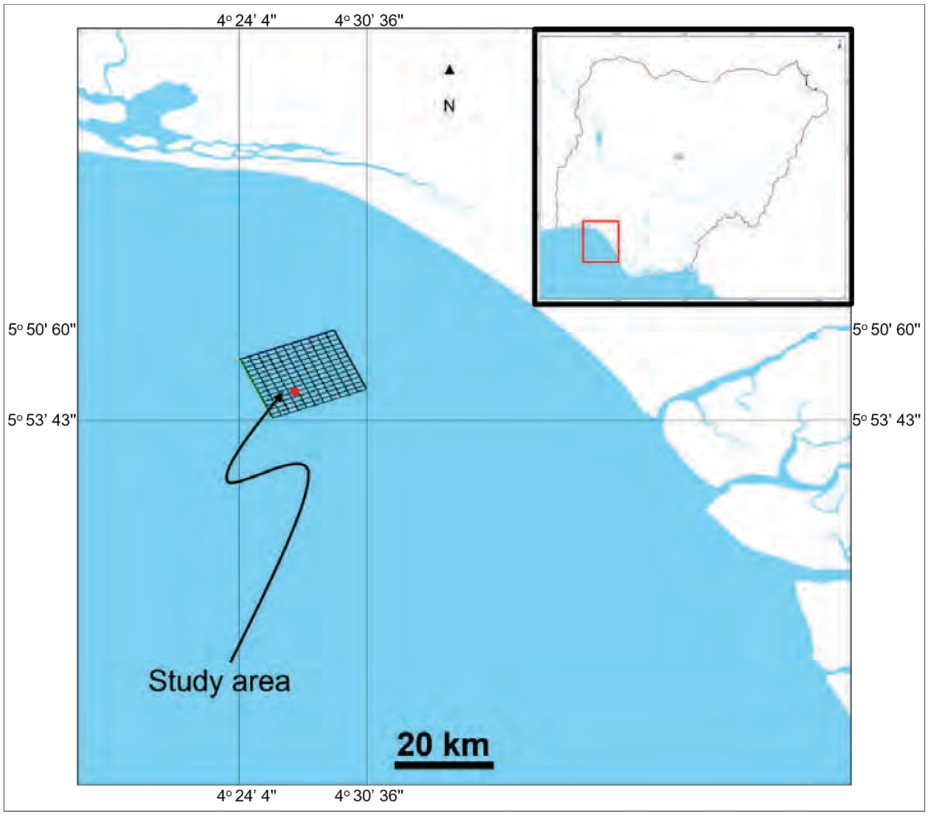


Figure 1: Location of study area within the western Niger Delta, Nigeria. Inset is the map of Nigeria. The slanted rectangular grid represents the coverage of the 3D seismic data and the approximate location of wells X and Y.

displayed in the bathymetric data, where ridges correspond to the crests of folds associated with faults, and low-lying areas align with piggyback basins that have formed above the rear portions of fault imbrications. The deepwater contractional segment of the Niger Delta can be divided into three primary zones, as detailed by Corredor *et al*. (2005): the inner fold and thrust belt, the outer fold and thrust belt, and the detachment fold zone. The Niger Delta is characterised by Tertiary marine and fluvial deposits, covering both oceanic crust and a portion of the African continental crust, as described by Bilotti and Shaw (2005). Deep wells drilled in this basin encounter a regressive sequence consisting of three lithostratigraphic units, namely, the Akata (the oldest), Agbada, and Benin Formations, as outlined by Short and Stauble (1967). During episodes of declining sea levels in the early to middle Miocene, the Niger Delta's shelf and slope experienced the formation of erosional canyons. These canyons, such as the Opuama canyon in the western Niger Delta and the Afam and Kwa-Ibo canyons in the eastern Niger Delta, have since become buried and filled with clay, making them particularly noteworthy, as documented by Doust and Omatsola (1990).

DATASETS AND METHOD

Biostratigraphic markers from well Y, located within the study area shown in Figure 1 was used for this work with the approval of the Nigeria Upstream Petroleum Regulatory Commission (NUPRC). Well Y data included foraminifera biostratigraphic picks and the corresponding

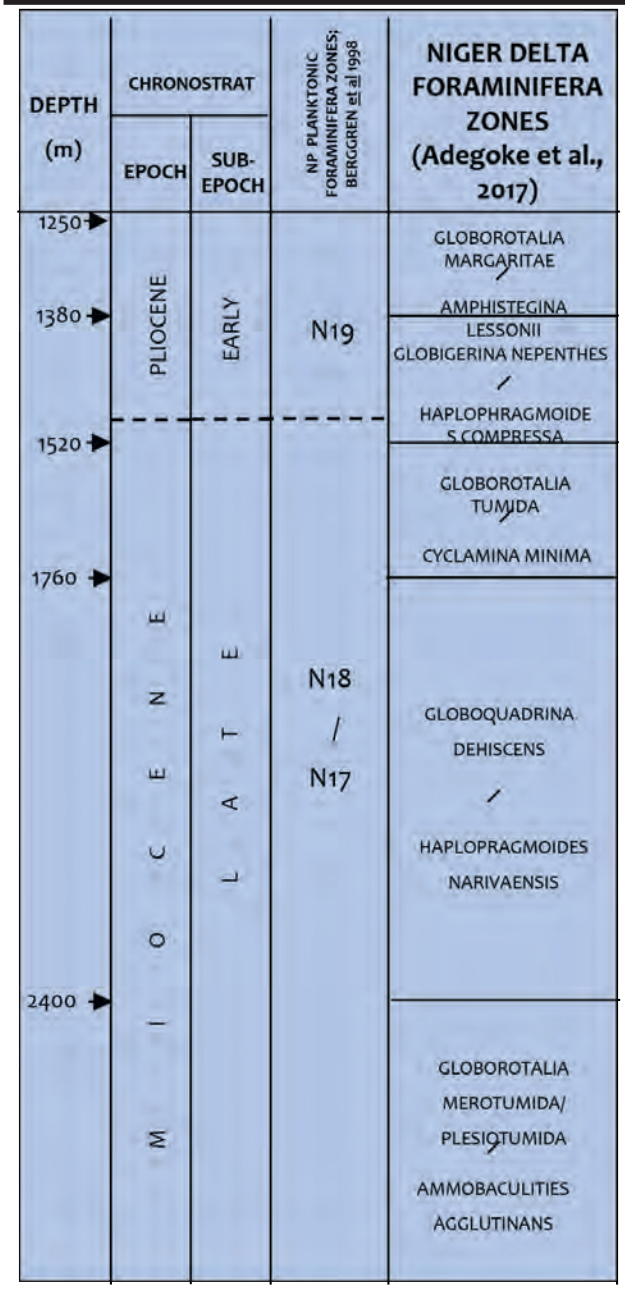


Figure 2: Stratigraphic column based on the integrated foraminifera markers from well Y. The oldest pick tied to the 3D seismic data is the G*loborotalia merotumida* (Miocene) while the youngest pick is the *Globorotalia margaritae* (Pliocene).

depths (Figure 2) along the well. The foraminifera data in the well covers only the deeper section (about 70%) of the entire 3D seismic vertical scale.

In addition to the biostratigraphic markers in well Y, the study was based on high-quality 3D seismic reflection data covering approximately 300 km^2 at a depth of around 500 meters in the deep offshore of the western Niger Delta (Figures 1 and 3). The seismic survey employed a vertical sampling interval of 4 milliseconds Two-Way Time (TWT), with inline and crossline spacing set at 12.5 meters. The seismic volume was migrated in time, not in depth. Therefore, true depths and stratal thicknesses were estimated using a clastic acoustic velocity of 2000 meters per second (for instance, 100 milliseconds TWT equates to 100 meters in depth). The data polarity follows the SEG (Society of Exploration Geophysicists) convention, where a blue reflection indicates an increase in acoustic impedance downward, while a brown reflection signifies a decrease in acoustic impedance downward, as shown in Figure 4.

Integration and Interpretation of Data

Using Petrel 2020 geological and geophysical software, the various biostratigraphic markers identified in well Y (Figure 2) were tied to the 3D seismic data (Figure 4) to identify mappable seismic horizons, and in turn helped to age-date the delineated seismic units. As the biostratigraphic data covers only part of the vertical scale of the 3D seismic data, the entire seismic interval was broadly splitted into two parts. The lower vertical segment that can be tied to available biostratigraphic data was tagged 'biostratigraphically-constrained' and the upper part without biostratigraphic picks was regarded as 'biostratigraphically-unconstrained'.

Each unit was defined by a base and a top seismic horizon and each top horizon's name was adopted for its seismic unit. Thus, the biostratigraphically-constrained interval was made up of the

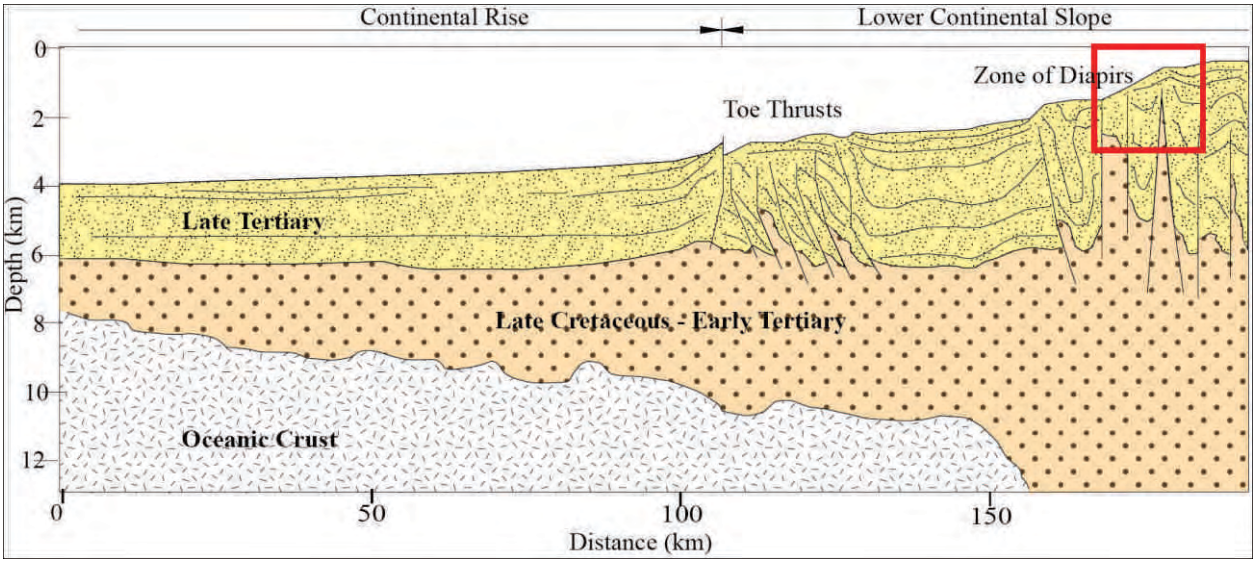


Figure 3: Regional dip transect across the Niger Delta showing the approximate location (red rectangle) of the study area (Modified from Lehner and De Ruiter (1977) and Doust and Omatsola, 1990).

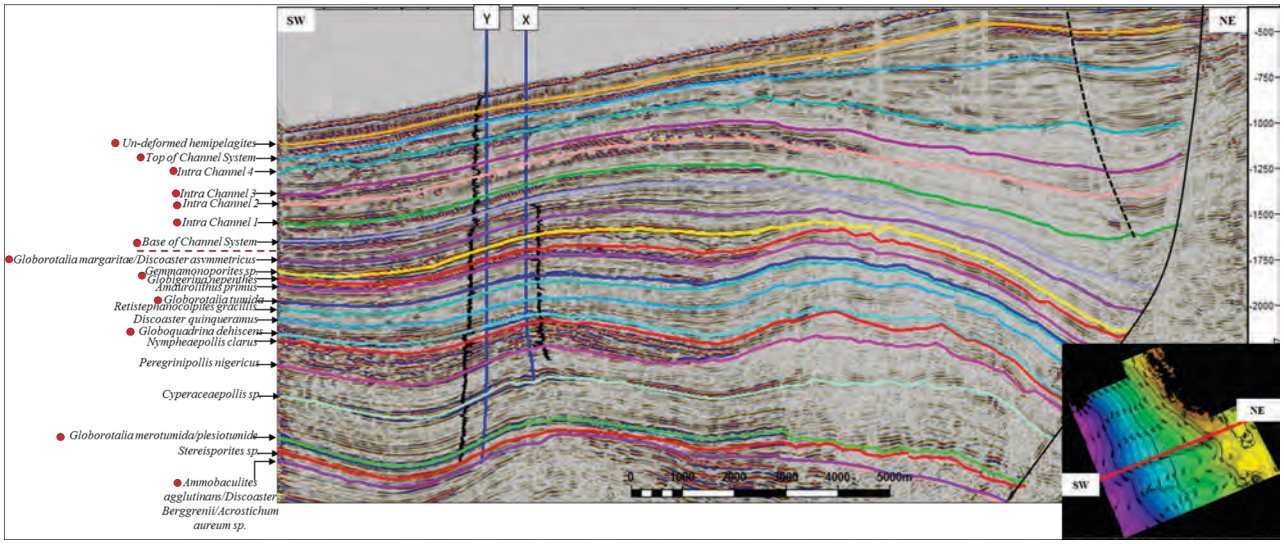


Figure 4: Dip orientated 3D seismic transect of the study area. The corresponding seismic horizons of the biostratigraphic markers from well Y are outlined. Note the vertical sub-division of the biostratigraphically-constrained and the -unconstrained intervals to the left-hand side. The red dots highlight the foraminera markers in this study.

Globorotalia merotumida (oldest), *Globoquadrina dehiscens, Globorotalia tumida, Globigerina nepenthes* and *Globorotalia margaritae* (youngest) seismic units. Also, the unconstrained seismic interval was informally deemed the 'interval of channel systems' as it was characterized by several spatial and vertical channels in the upper regime of the stratigraphy. This interval was then splitted into six seismic units by seven key seismic horizons. These, from the interval base to its top, are 'Base of channel system' (oldest), 'Intra channel 1', 'Intra channel 2',

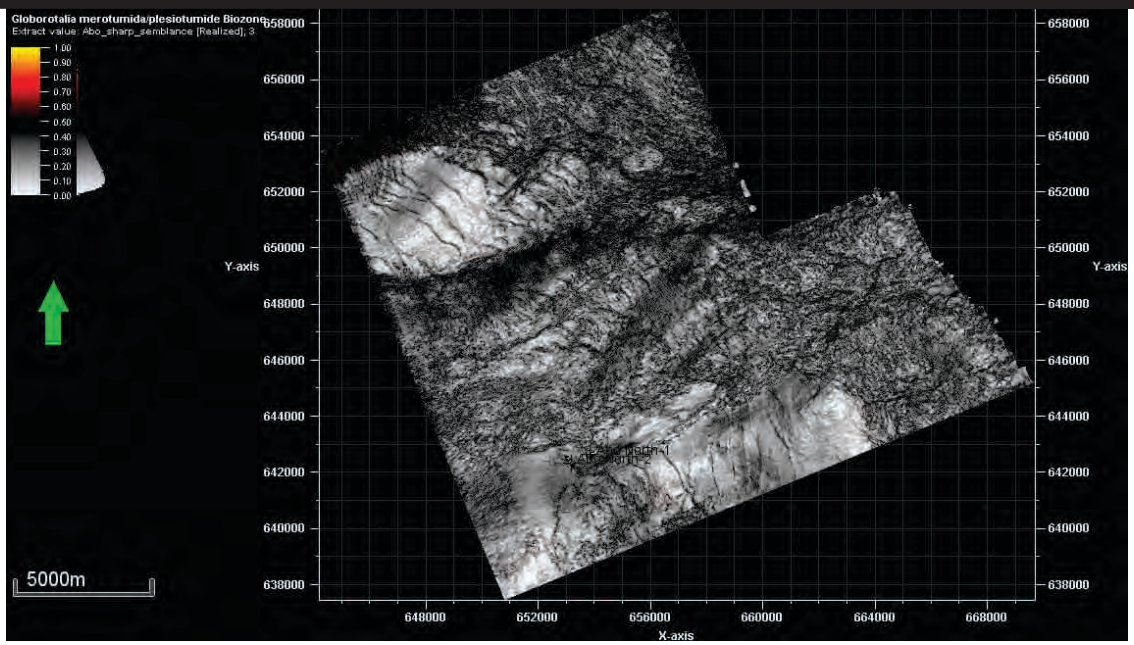


Figure 5: Semblance map of the *Globorotalia merotumida* seismic unit. The unit indicates a widespread representation of highly disaggregated, chaotic flows.

'Intra channel 3', 'Intra channel 4', 'Top of channel system', and 'Undeformed hemipelagites' (youngest) (Figure 4).

Each identified seismic horizon was conventionally mapped and fully interpreted line by line across the entire 3D seismic data wall-to-wall. The inferred horizons were then gridded to obtain a continuous subsurface map for each of the surfaces. The interval thickness maps of the seismic units were obtained by subtracting the respective horizon tops from the horizon bases. Additionally, the 3D seismic data was conditioned into semblance attribute to enable the respective semblance to be extracted along the interpreted surfaces for the generation of semblance map

RESULTS AND SYNTHESIS

This section comprises the descriptions of the features identified for the individual seismic units as defined by their base horizon and top horizon. The internal seismic facies is described based on the sub-regional seismic cross section in Figure 4 and spatial occurrences of sediment gravity flows are characterized using the semblance attribute maps, the TWT topographic maps, and the relative acoustic impedance (RAI) maps. Some sedimentological inferences and deductions were made in relation to existing in similar slope environments.

Globorotalia merotumida Seismic Unit

This unit overlies the *Ammobaculites agglutinans* horizon (Figure 4) and its top is the *Globorotalia merotumida* horizon. The internal seismic facies is characterised by low amplitude moderately chaotic facies at the base (Figure 4) and laterally continuous high amplitude reflection at the top. From the disaggregated seismic character and signatures, this unit is inferred to be a debris flow capped by sandy turbidites. The debris flow interpretation is further supported by the largely

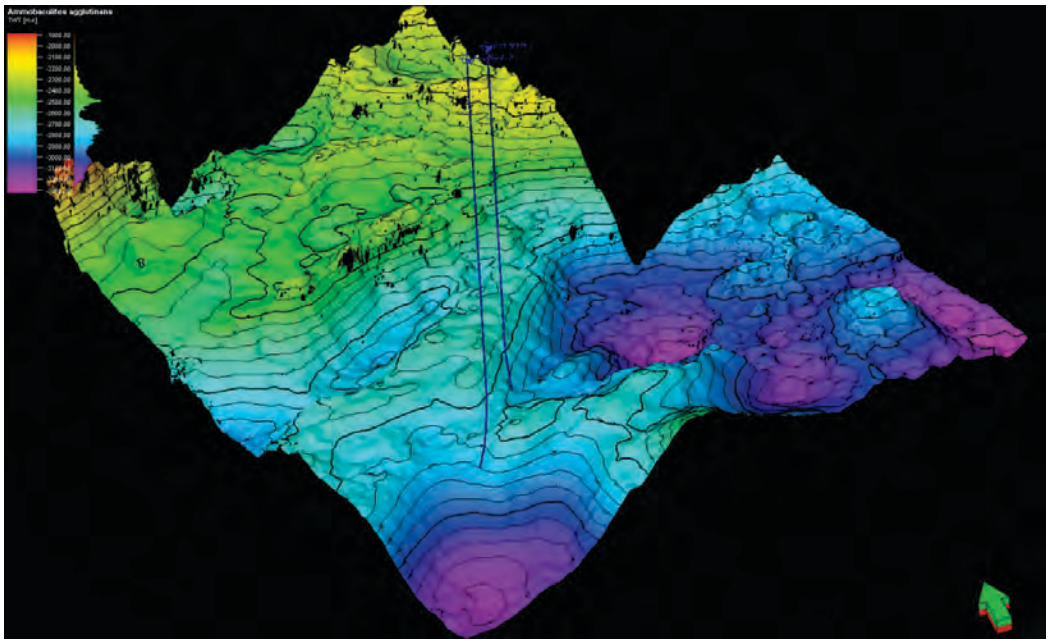


Figure 6: 3D perspective view of the *Ammobaculites agglutinans* surface mapshowing the presence of several mini basins that functioned as the receptacles for the deposition of the overlying *Globorotalia merotumida* seismic units.

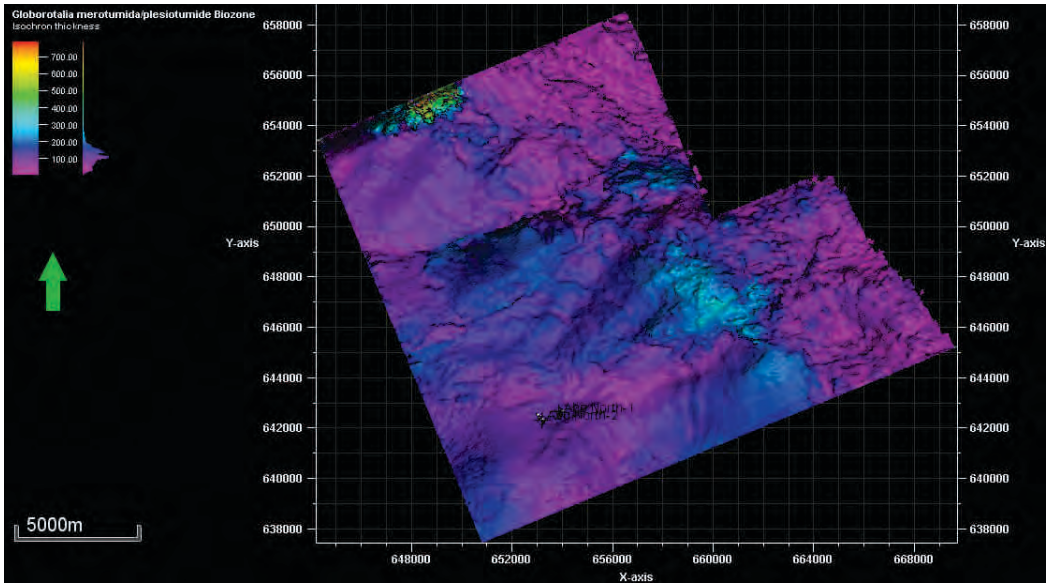


Figure 7: Thickness map of the *Globorotalia merotumida* seismic unit. The localized thicker packages to the east, about 300m, coincide with the development of the mini basin in the 3D topographic visualization.

chaotic character indicated in the *Globorotalia merotumida* semblance map (Figure 5). Debris flow is often shed off when the receiving mini-basin is above grade (i.e., when topographic relief across the basin is high) as indicated in Figure 6 where several occurrences of mini basins dotted the surface of the *Ammobaculites agglutinans* horizon. Debris flow occupy stratigraphic regime of this nature where slope instability creates different episodes of mass transport deposits

(Booth *et al.,* 2000; Olafiranye *et al.,* 2013).

Based on the thickness scale (colour bar at the top left-hand corner of Figure 7), the unit's thickness varies between 100 and 300 m across the study area. The localized thicker packages, about 300 m, coincide with the mini basins identified in Figure 6.

Globoquadrina dehiscens Seismic Unit

This unit has *Globorotalia merotumida* and the *Globoquadrina dehiscens* seismic horizons respectively at it base and top. At its base, the seismic facies displays largely laterally continuous low amplitude with rare high amplitude discontinuous reflectors (Figure 4). It changes at the top to moderately high amplitude, dotted by low amplitude. This unit is interpreted as a hemipelagic deposit with sandy turbidites and heteroliths of a turbidite system at the top (Rebesco and Stow, 2001; McHargue, 1991).

The *Globoquadrina dehiscens* unit semblance map (Figure 8) shows the subtle spatial variability in the unit's seismic facies. The red dashed line points to the facies difference in the unit which indicates that variations exists and points to possible lithologic heterogeneities within the unit.

Its mean thickness is about 500 m. It thins northwestwards to 250 m and about 100 m in its north (Figure 9). Its thickest part (up to 900 m; Figure 10) arose from filling of a large mini basin (Figure 9) that pre-existed the *Globoquadrina dehiscens* unit's deposition.

Globorotalia tumida Seismic Unit

The *Globorotalia tumida* stratigraphic unit is bordered at the base by the *Globoquadrina dehiscens* seismic horizon and at the top by the *Globorotalia tumida* horizon (Figure 4). It is characterised by laterally continuous low to

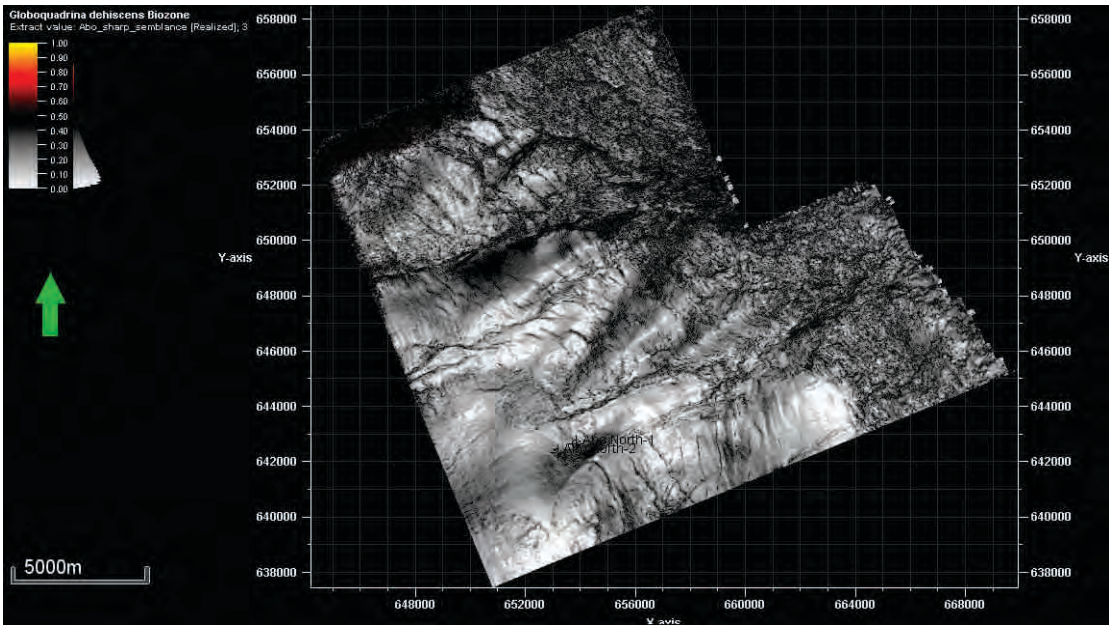


Figure 8: Semblance map of the *Globoquadrina dehiscens* seismic unit. The seismic unit shows clear spatial variation, possibly lateral heterogeneities from upslope in the north to downslope in the south.

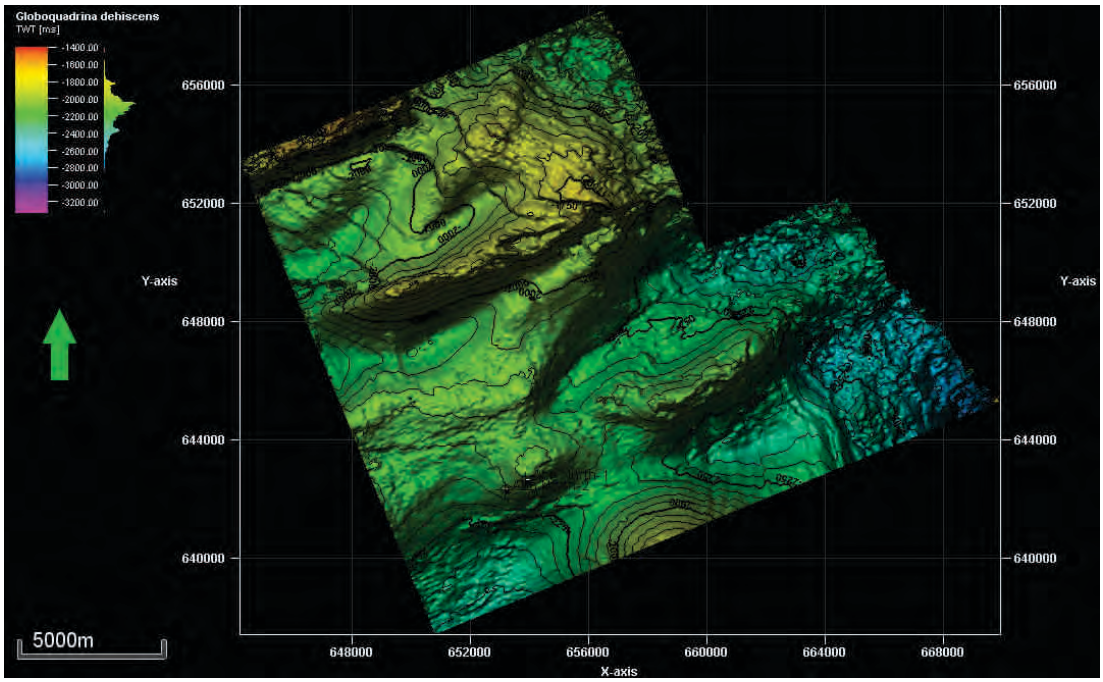


Figure 9: Surface map of the *Globoquadrina dehiscens* horizon indicating the large pre-existing mini basin in the north which resulted in about 900 m thickness. Other mini basins also exist on the surface.

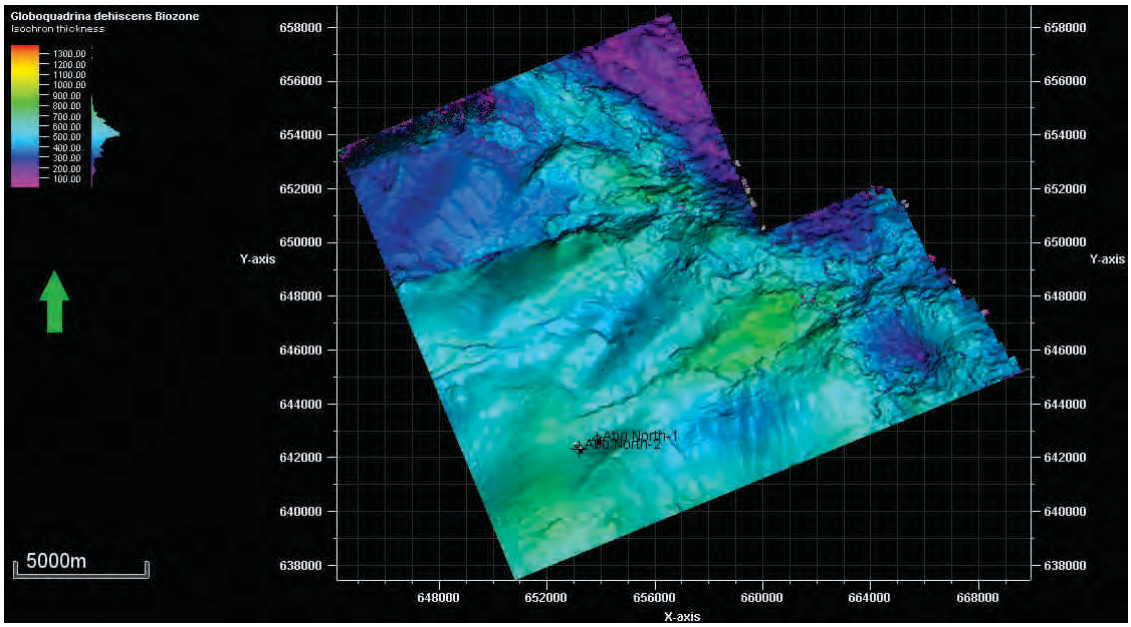


Figure 10: Thickness map of *Globoquadrina dehiscens* seismic unit. The unit's thickness varies between 100 and 900 m of sediment gravity flows.

moderate amplitude at the base and low amplitude poorly continuous facies at top. This is interpreted to represent normally graded turbidite deposit at the base and debris flow at the top (Armitage *et. al.,* 2009; Jackson and Johnson, 2009; Armitage and Stright, 2010; Olafiranye *et. al*., 2013). In the semblance map of the *Globorotalia tumida* stratigraphic unit, facies variability (Figure 11; see red dash line) appears to mimic topographic controls (Figure 12) where high semblance facies upslope occurs on the topographic high and the low semblance downslope within the topographic low. This implies that the interpreted low amplitude and laterally continuous hemipelagites sub-unit was deposited within the topographic low whereas the low amplitude poorly continuous debris flow occupies the topographic highs.

From the colour bar of the thickness map (Figure 13), the thickness of the unit differs across the area and varies between 100 – 200 m. The thicker part is widespread in the northern part of the area where deep mini basins relief up to 1300 m (Figure 12) previously existed to act as the repository for the deposit.

Globigerina nepenthes Seismic Unit

The base and top of this unit are marked by the *Globorotalia tumida* and *Globigerina nepenthes* seismic horizons (Figure 4). The seismic facies at the base of the unit are composed of high amplitude reflections interspersed by low amplitude chaotic facies. The top is represented by high amplitude reflection laterally wiggly facies (Figure 4). This facies occurrence is interpreted as episodes of debris flow and turbidites deposition at the base whereas the top of the unit represents sandy slump deposit (Sawyer *et al*., 2007; Alves, 2010; Omosanya and Alves, 2013). The semblance map (Figure 14) shows prevalence of debris flow-related deposits within this stratigraphic unit. This widespread debris flow is pervasive in the area except the western part. It can be inferred from this observation that the debris component of this unit was deposited in the

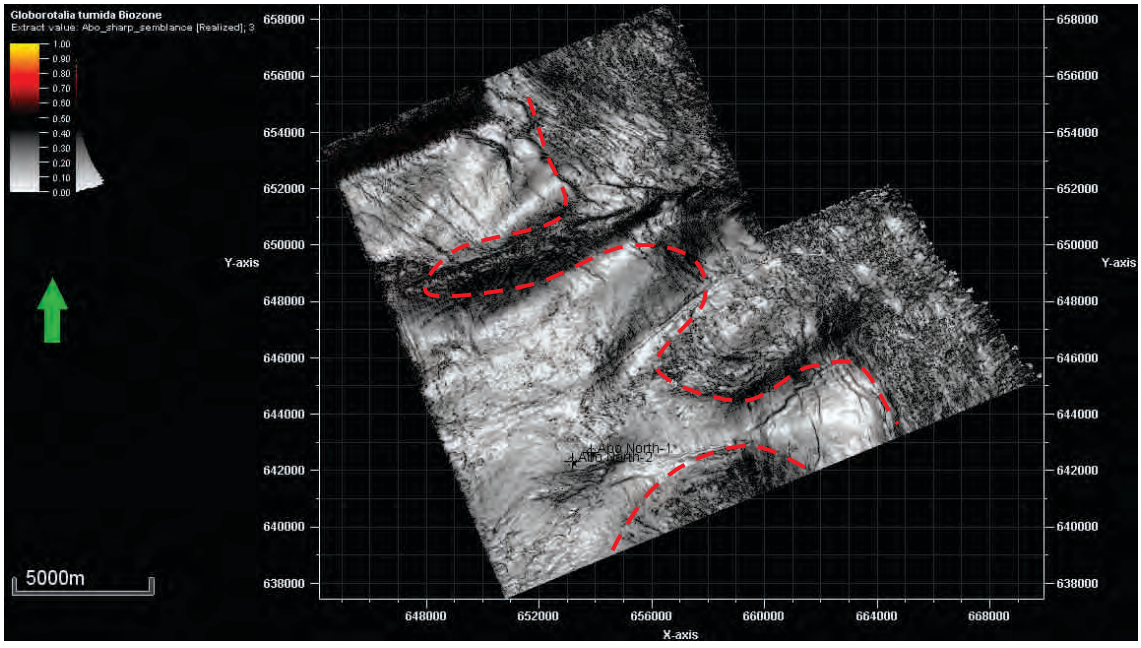


Figure 11: Semblance map of the *Globorotalia tumida* seismic unit.

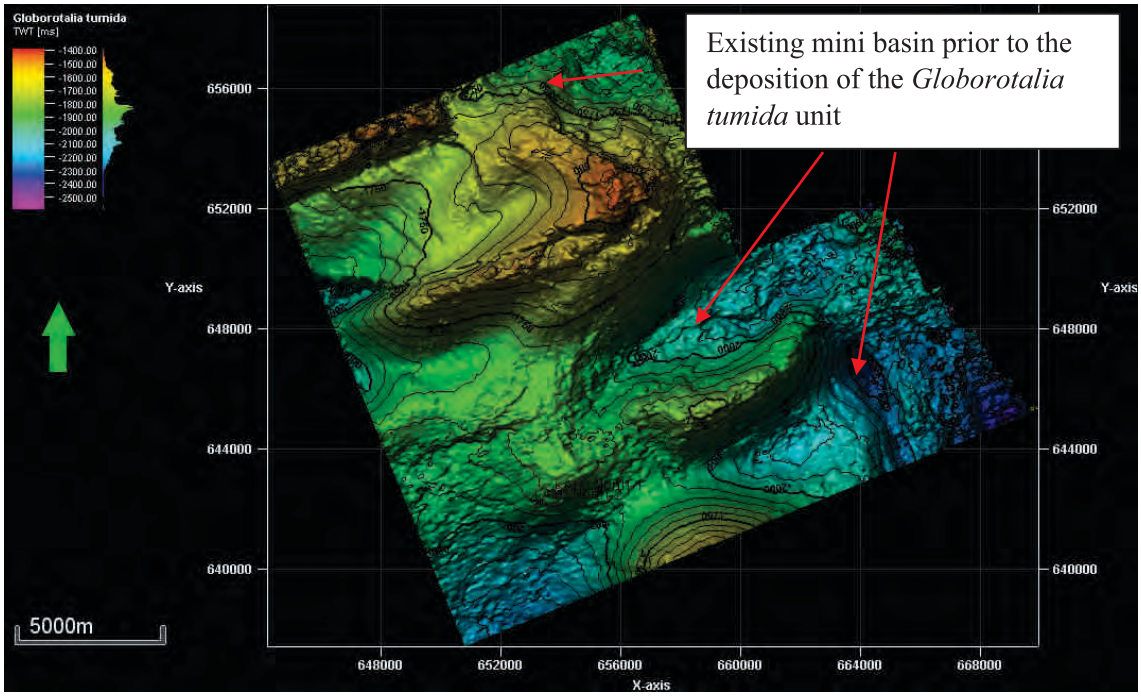


Figure 12: Surface map of *Globorotalia tumida* seismic unit.

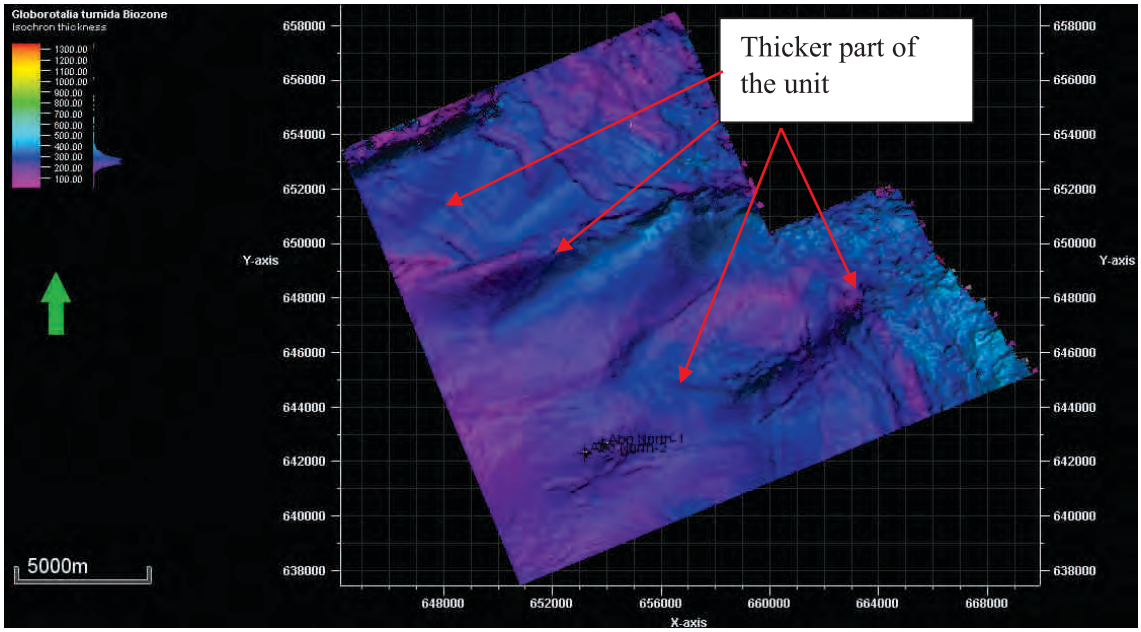


Figure 13: Thickness map of *Globorotalia tumida* seismic unit.

proximal part of the basin whereas the turbidites sub-unit extended further offshore into the distal part of the area (Walker, 1967; Jackson *et al*., 2009). Although there is relative reduction in the number of identified mini basins (Figure 15) compared to the underlying units, large and high relief topography persist during the deposition of the *Gobigerina nepenthes*

.The thickness of the deposit varies between 100 and 300 m distributed across the study area with places of precursor high topography corresponding to the thicker part of the unit and points of low topography received thinner deposit (Figures 15 and 16). As this relationship is

converse to expected norm where thicker sediment is expected within topographic lows to form constructive canyons (Posamentier and Walker, 2006; Straub and Mohrig, 2008; Straub and Mohrig, 2009; Straub *et al.,* 2008; Straub *et al.,* 2012), it can be suggested that the period of

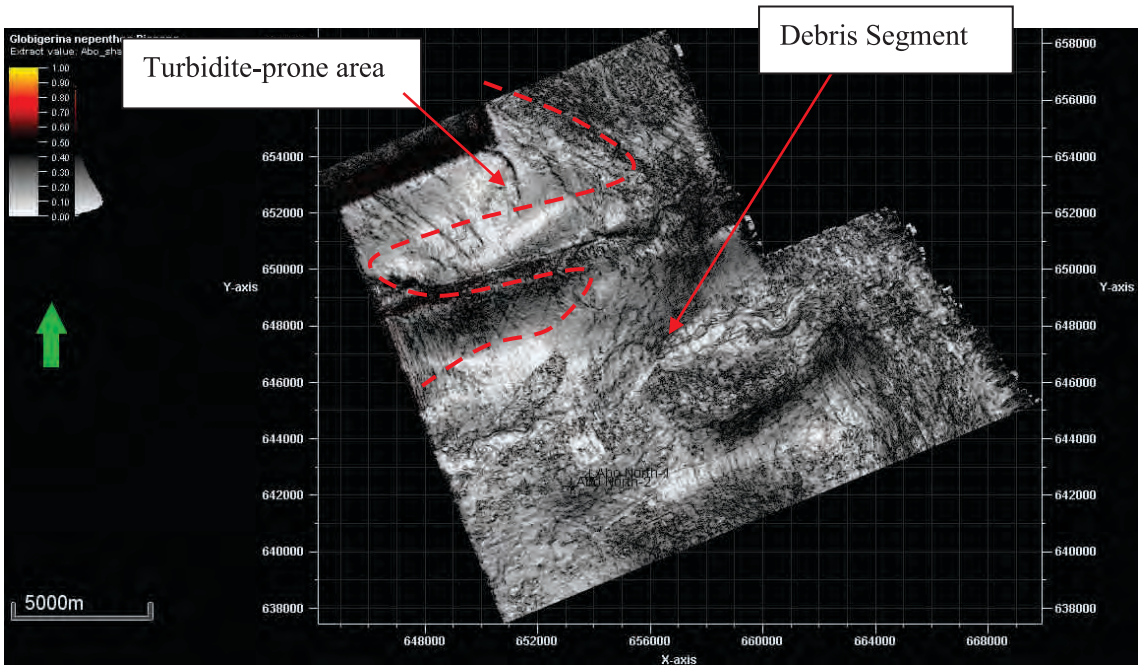


Figure 14: Semblance map of *Globigerina nepenthes* seismic unit. The chaotic high semblance is pervasive in the proximal area except the western part, while the low semblance facies is in the distal western limit.

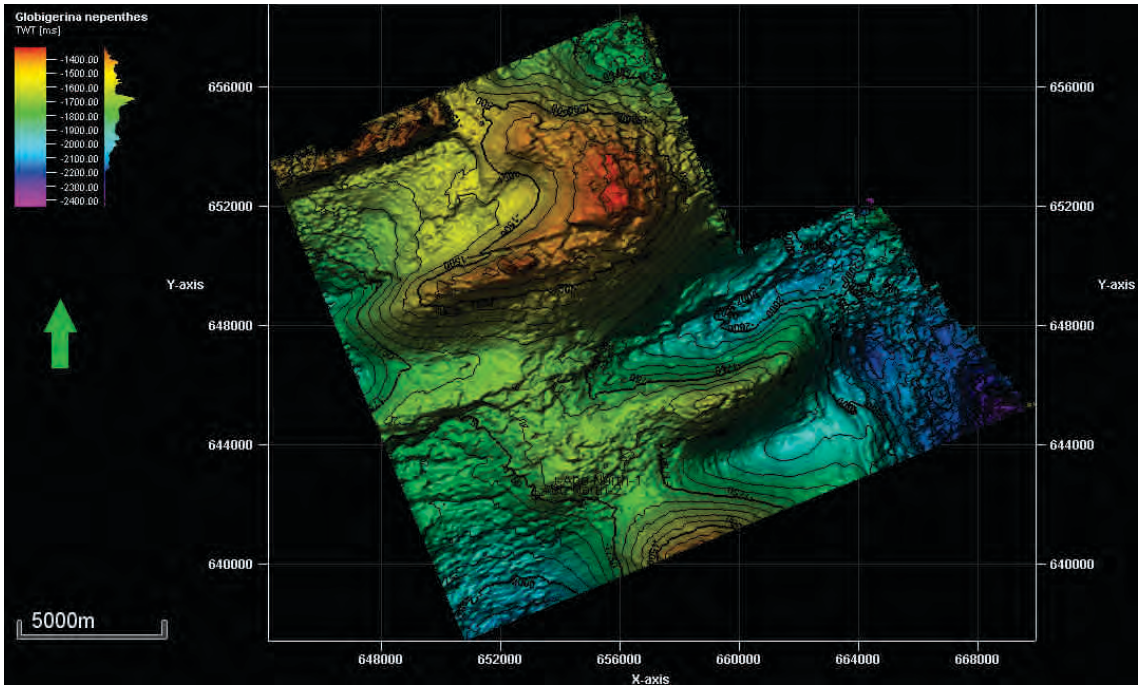


Figure 15: Surface map of *Globigerina nepenthes* horizon. Notice the relative reduction in the number of mini basins, but large sizes persist.

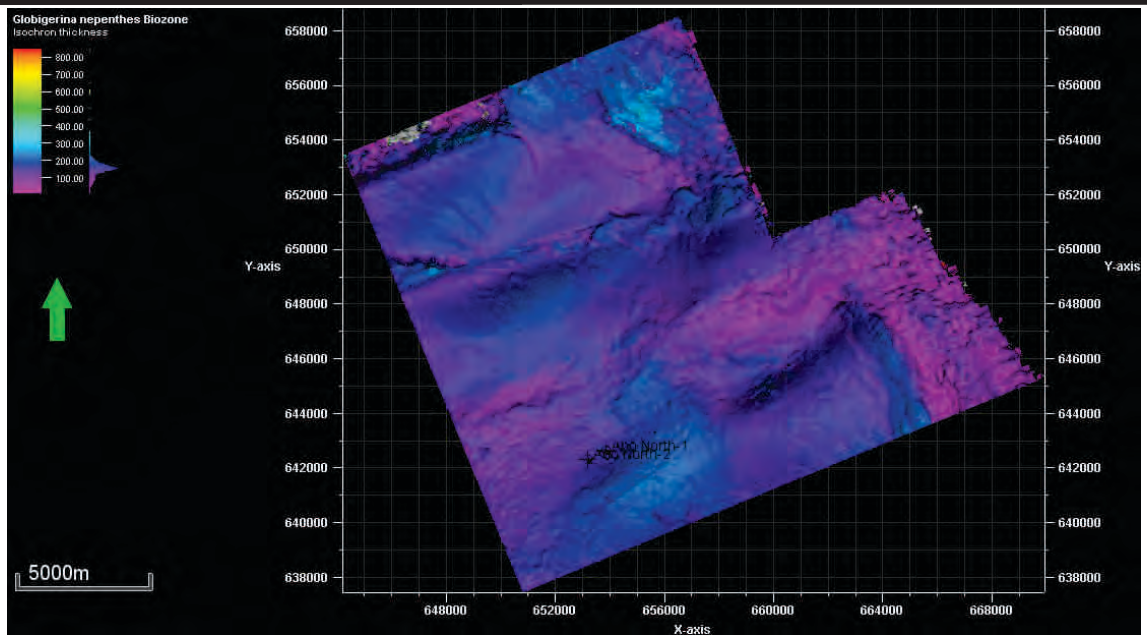


Figure 16: Thickness map of *Globigerina nepenthes* seismic unit. The thickness of the deposit varies between 100 and 300 m distributed across the study area with places of precursor high topography corresponding to the thicker part of the unit and points of low topography received thinner deposit.

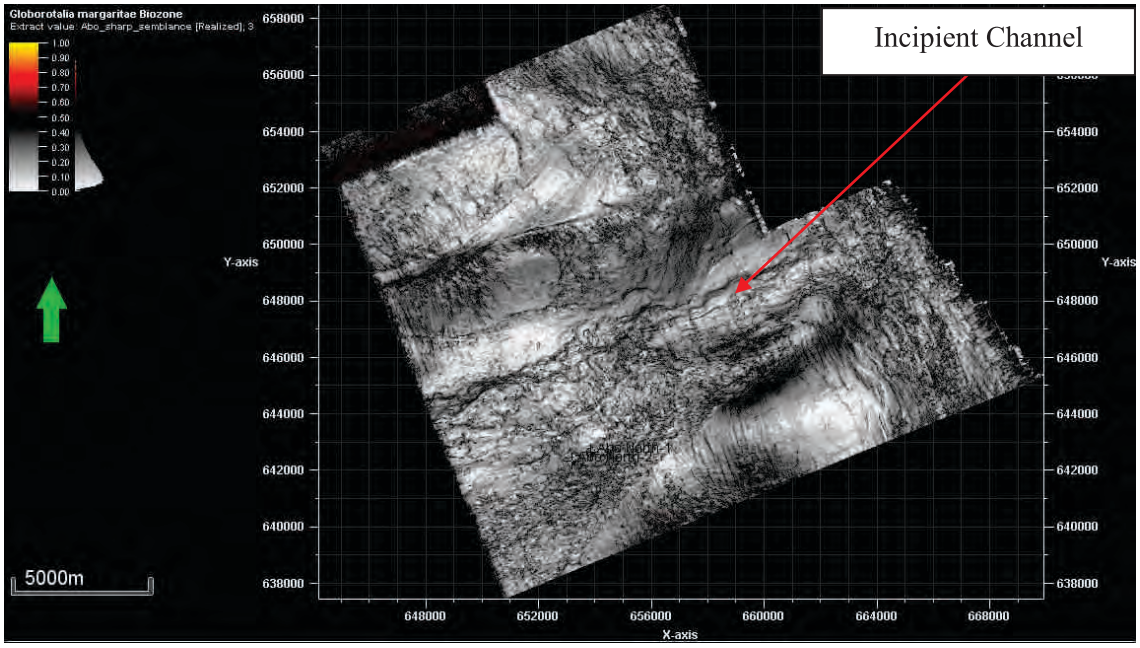


Figure 17: Semblance map of *Globorotalia margaritae* seismic unit.

deposition of the *Globigerina nepethens* unit was marked by intermittent erosion of the deposits within the topographic lows (Macdonald *et al*., 2011).

***Globorotalia margaritae* Seismic Unit**

The base of this unit is represented by *Globigerina nepenthes* seismic horizon and the unit is capped by the *Globorotalia margaritae* seismic horizon (Figure 4). At the base, it is characterised

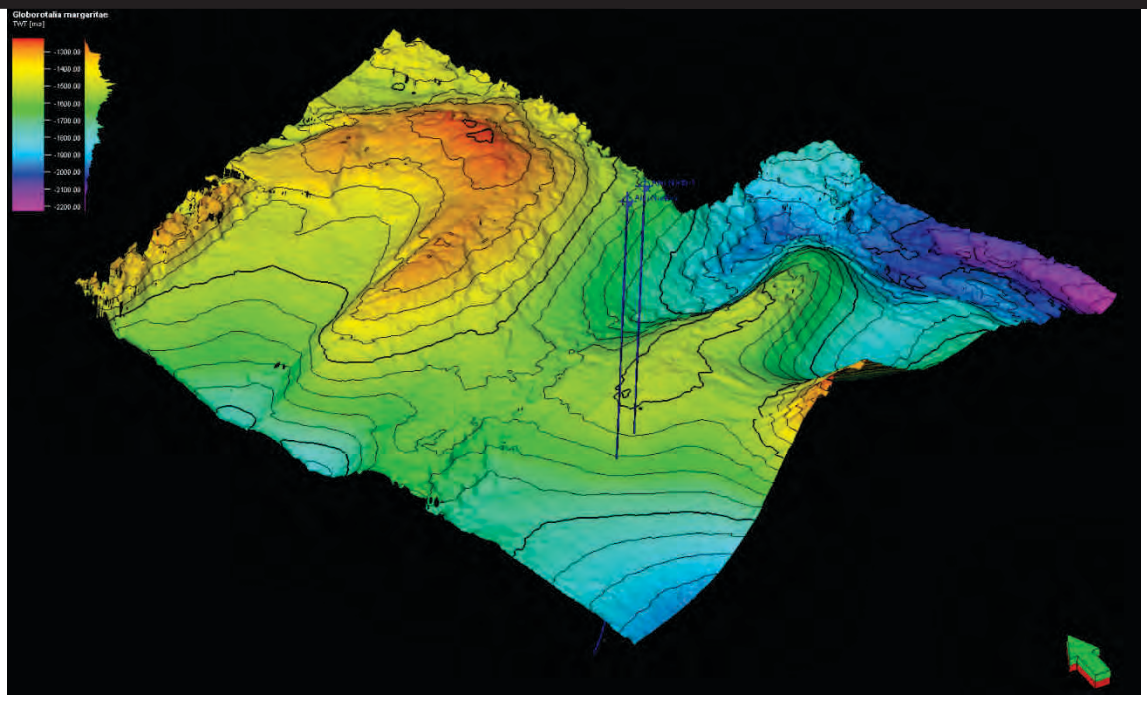


Figure 18: 3D visualization of the surface map of *Globorotalia margaritae* seismic unit.

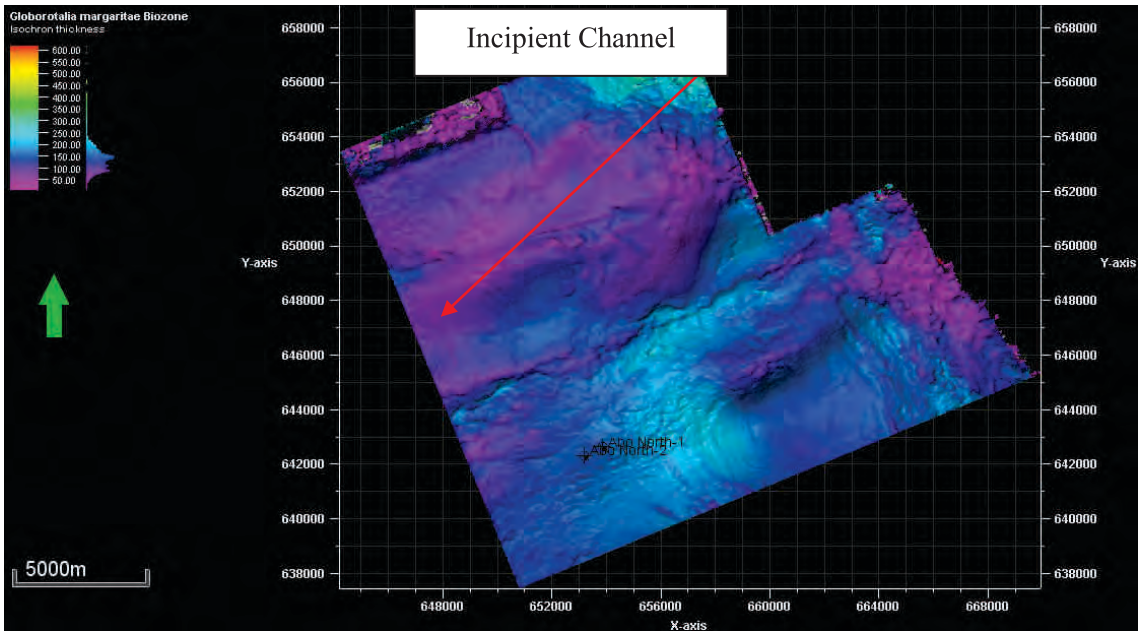


Figure 19: Thickness map of *Globorotalia margaritae* seismic unit.

predominantly by low amplitude package which encased a high amplitude reflection. The top of the unit is represented by high amplitude facies which passes laterally to low amplitude. The basal sub-unit is interpreted to be an embedded sandy unit within hemipelagites while the top is considered to be composed of turbidites deposited under a waning energy regime (Armitage *et al*., 2009; Jackson *et al*., 2009; Olafiranye *et al*., 2013). The semblance map (Figure 17) of the *Globorotalia margaritae* stratigraphic unit generally indicate minor facies variation within the unit despite

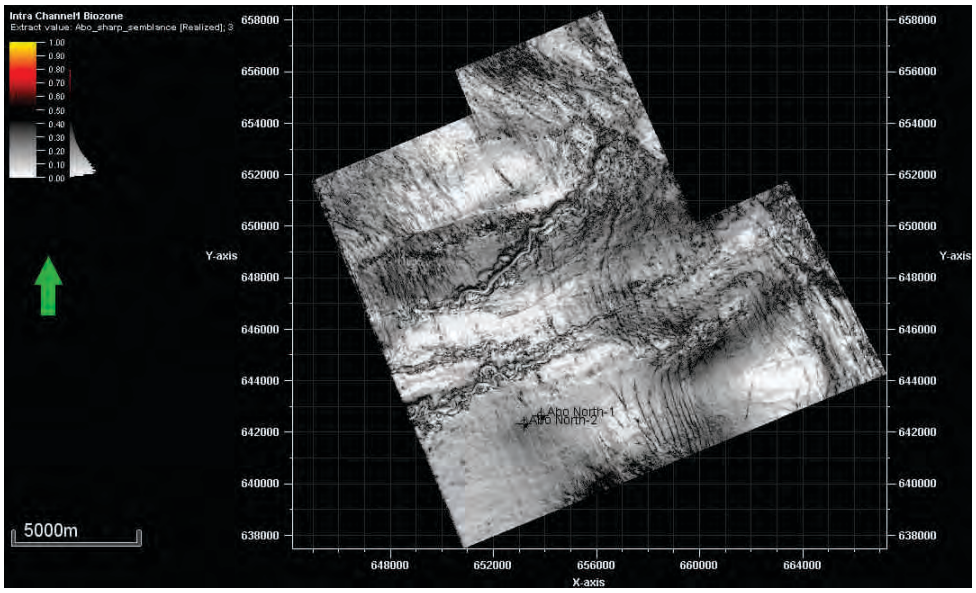


Figure 20: Semblance map of 'Intra channel 1' stratigraphic unit. Two channels developed in an approximately northeast-southwest trend and acted as sediment fairways for sediment gravity flows that have been shed off from the upslope area.

appreciable existence of topographic relief (Figure 18). However, a closer observation of the semblance map shows that the precursor channel is present and maintains the northeast to southwest trend during its emergence in the *Globorotalia tumida* stratigraphic unit.

The thickness of the *Globorotalia margaritae* seismic unit is up to 400 m in the thicker part of the area and reduces to about 100 m in the thinner part (Figure 18) where the ancestral mini basin at the initial stage of deposition (Figures 7 and 19) have been filled by sediment gravity flows.

Intra Channel-1 Seismic Unit

The base of the Intra Channel-1 stratigraphic unit is represented by the seismic horizon which is informally termed 'Base of channel system' because this event marked the temporal beginning of the development of the channel system in the upper section of the 3D seismic data (Figure 4). The stratigraphic unit is topped by the 'Intra channel 1' seismic horizon. The internal seismic facies makeup of the unit is characterised by low amplitude continuous reflections at the base and passes to high amplitude continuous reflections at the top (Figure 4). This is interpreted as turbidites deposits. The semblance map of the 'Intra channel 1' unit (Figure 20) shows that the unit is largely uniform with some high semblance chaotic facies to the northwest. The updip chaotic part mark the upslope head of a channel system which terminates downslope to the south (Figure 20). A wider (2000 m wide) more sinuous channel developed further south. These two channels served as the migration pathway or sediment fairway for sediment gravity flows that have been shed off from the upslope area.

The existence of the southern channel within this stratigraphic unit is further confirmed in 3D topographic visualisation as shown in Figure 21.

The stratigraphic unit is up to 350 m thick in the eastern part of the study area and about 25 m thick in the West. The wider channel influenced

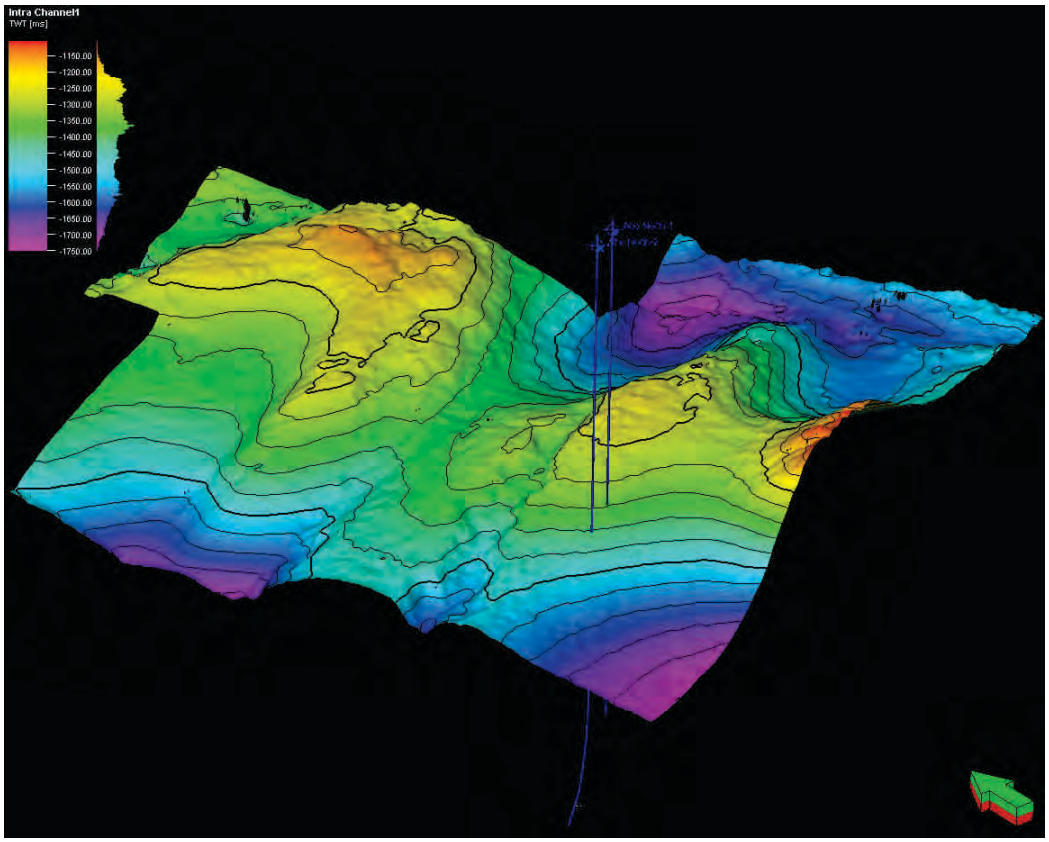


Figure 21: 3D visualization of the surface map of 'Intra channel 1'. Note the development of a channel which is pronounced to the south of the surface.

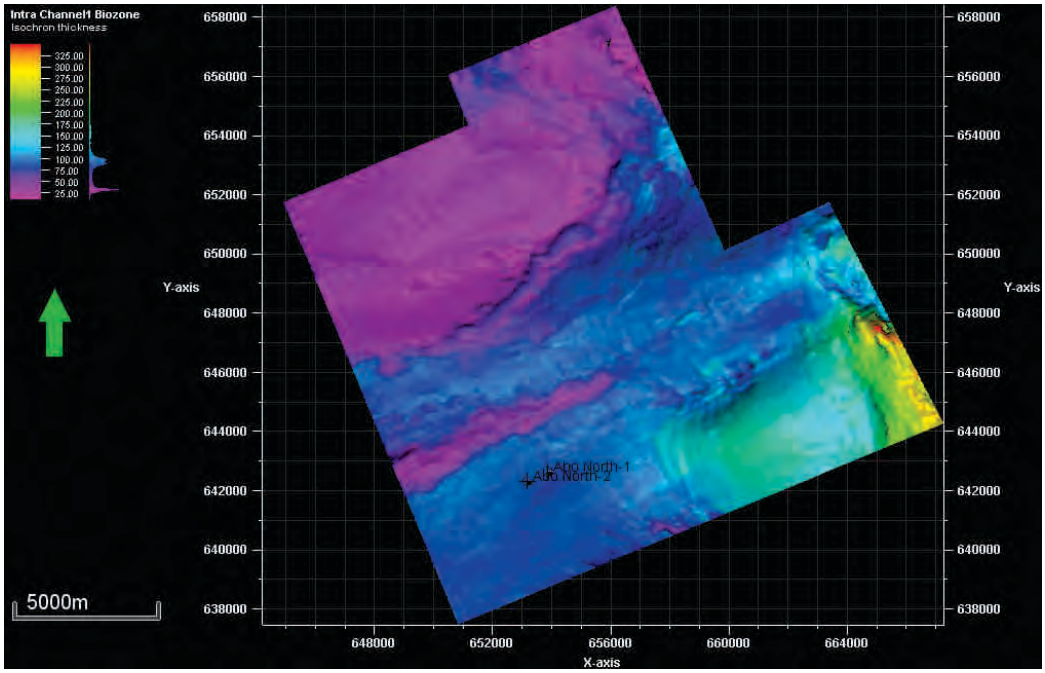


Figure 22: Thickness map of Intra channel-1 seismic unit. The unit is about 350 m thick to the east. Also, note the 25 m thickness of the unit with a northeast-southwest trend.

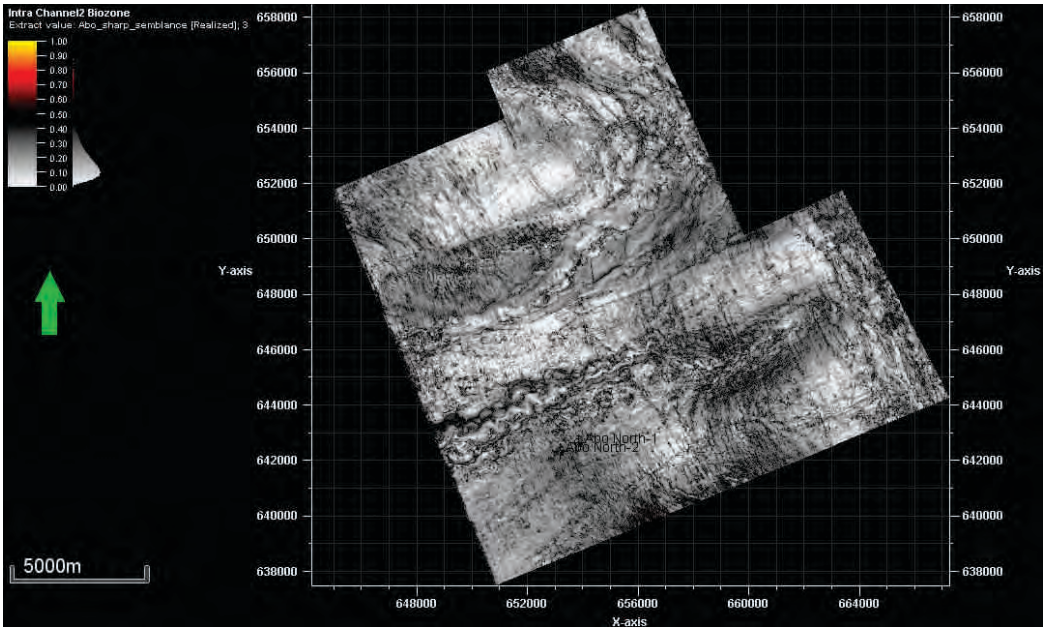


Figure 23: Semblance map of 'Intra channel 2' seismic unit. The semblance character is generally low and almost uniform. There is some level of sinuosity within the channel.

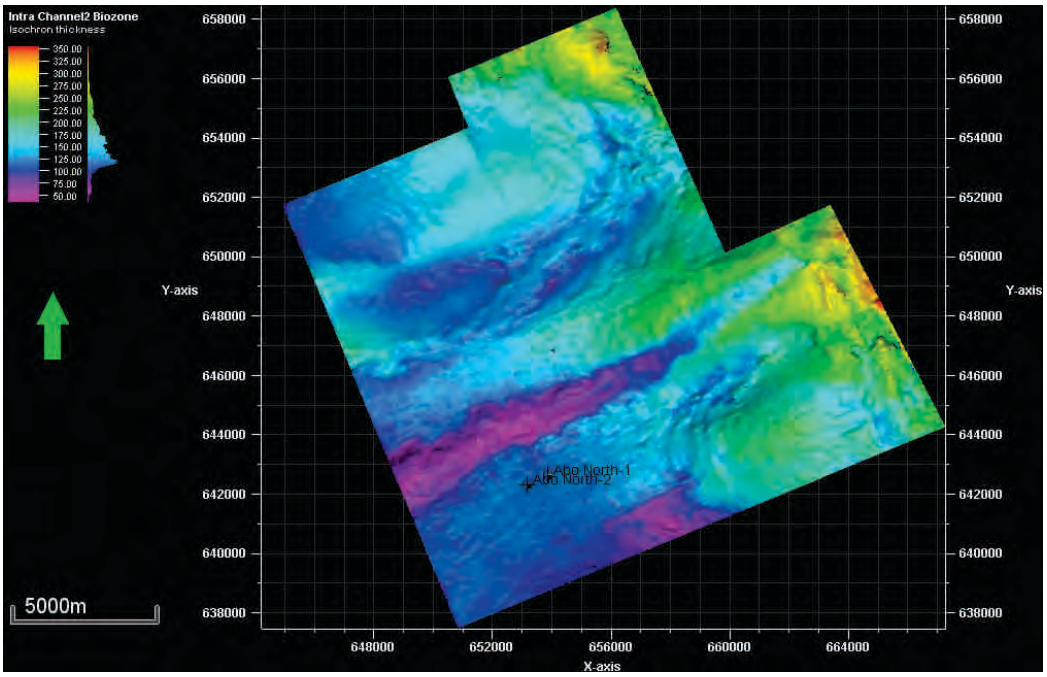


Figure 24: Thickness map of 'Intra channel 2' stratigraphic snit. Note the thinner part (approximately 50 m) which mimics the morphology of the NE-SW canyon.

sediment thickness of about 25 m (Figure 22) within is stream with up to 80 m thickness at its banks.

Intra Channel-2 Seismic Unit

The base of the 'Intra channel 2' stratigraphic unit is represented by the 'Intra channel 1' seismic horizon and its top is marked by the 'Intra channel 2' seismic horizon (Figure 4). It is typified dominantly by low amplitude laterally continuous

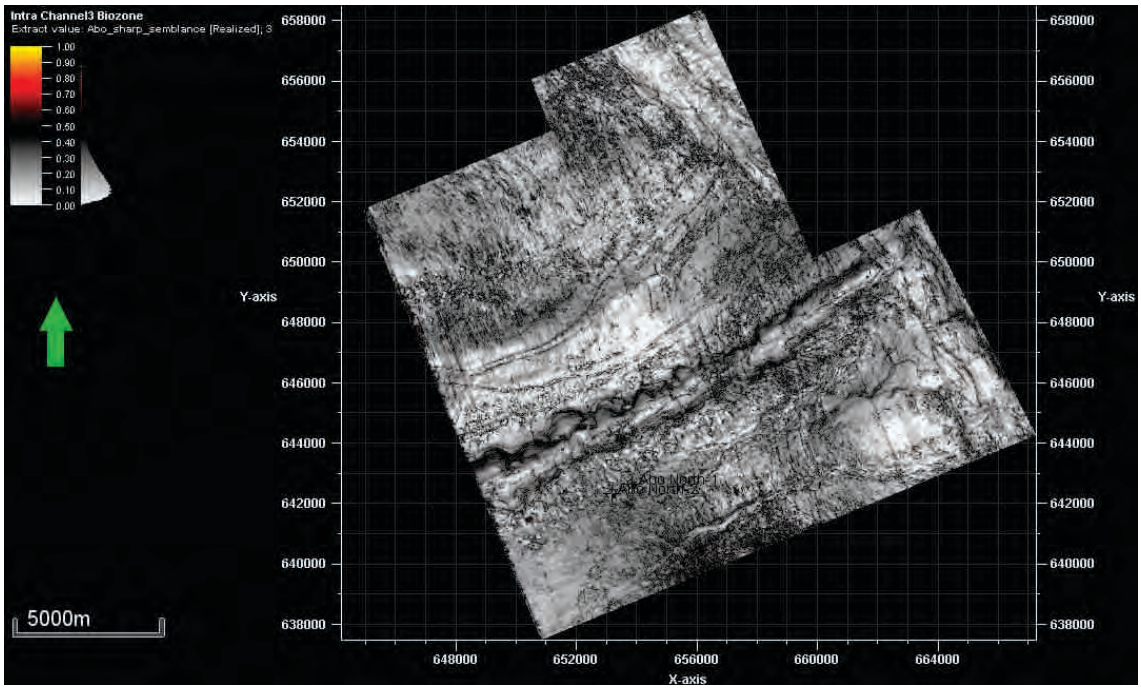


Figure 25: Semblance map of 'Intra channel 3' seismic unit. Note the pronounced northeast-southwest trending feature which indicated that the ancestral channel was still active with its position aligned with the underlying linear feature.

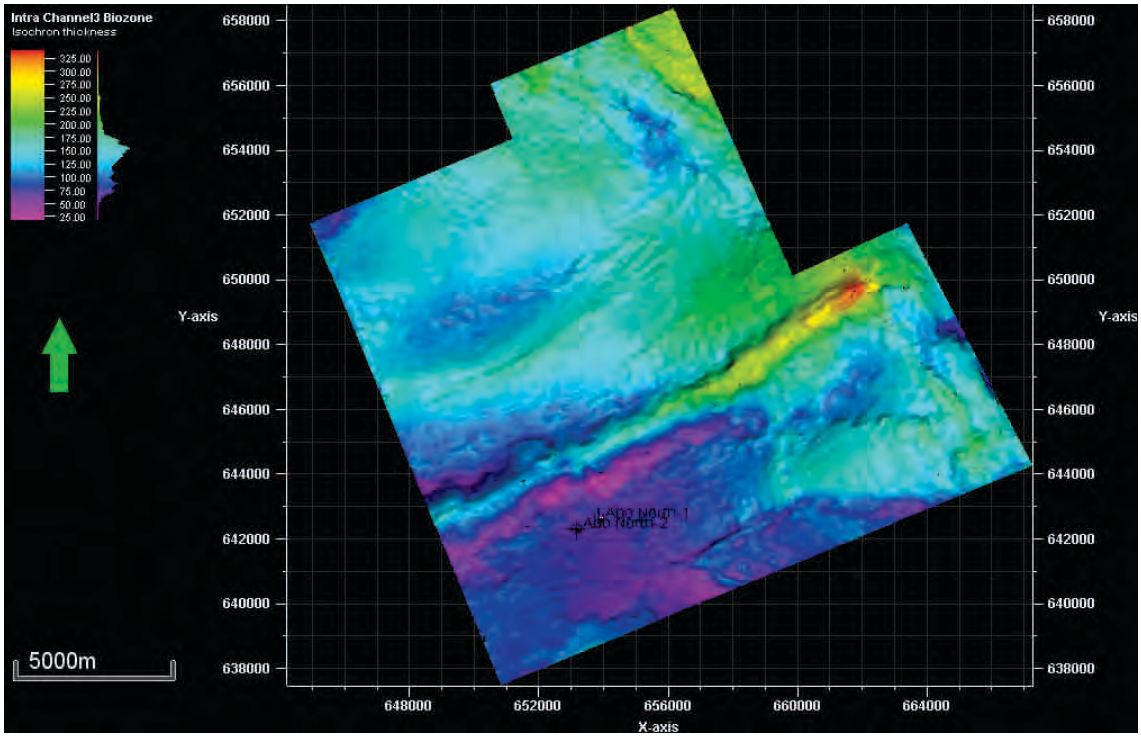


Figure 26: Thickness map of Intra channel 3 seismic unit. The centre has a northeast-southwest trending feature (175 m and 300 m thick to the southwest and northeast respectively).

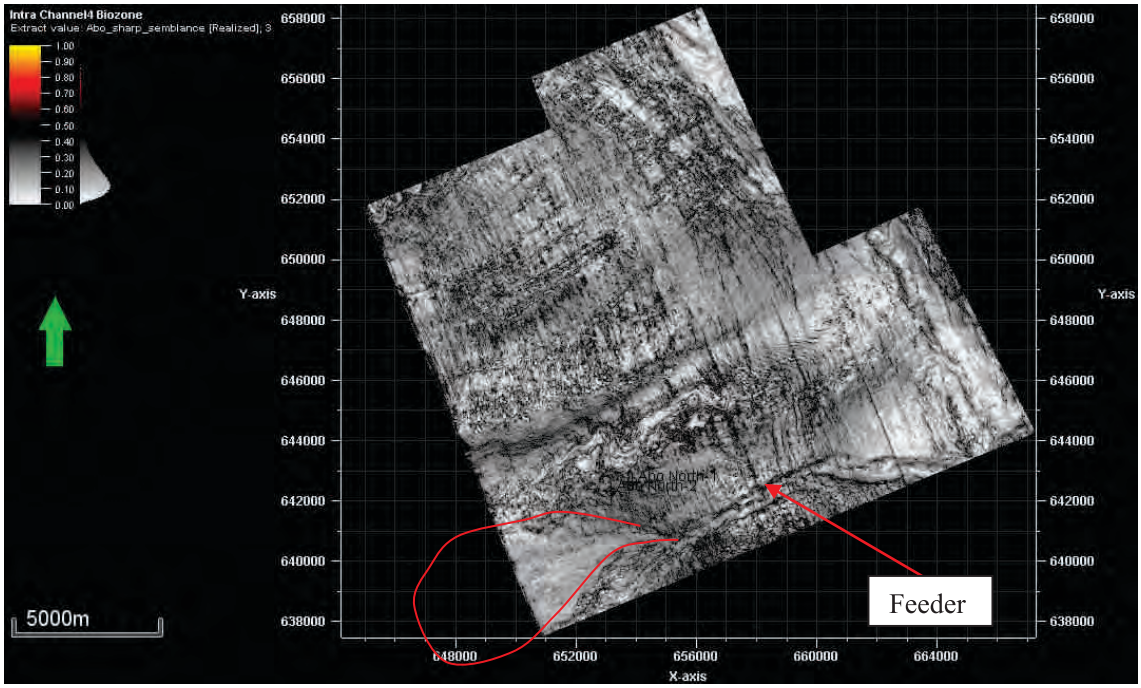


Figure 27: Semblance map of 'Intra channel 4' seismic Unit. The facies are largely similar across the unit. However, the southernmost part denoted by a red oval line has a different lower semblance than other areas. This lobe-like feature is considered to represent a slope fan.

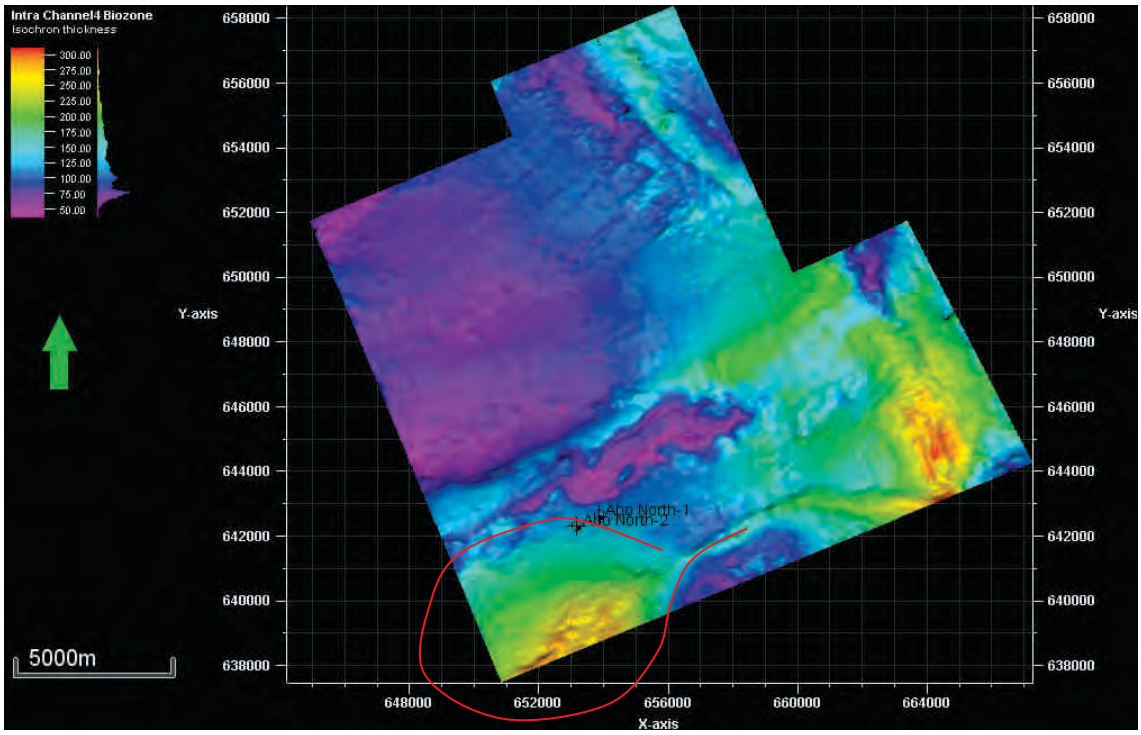


Figure 28: Thickness map of 'Intra channel 4' seismic unit. The lobate feature at the southernmost tip represents a slope fan formed by the funneling of sediment gravity flows through the adjoined feeder which is connected to a staging area in the east.

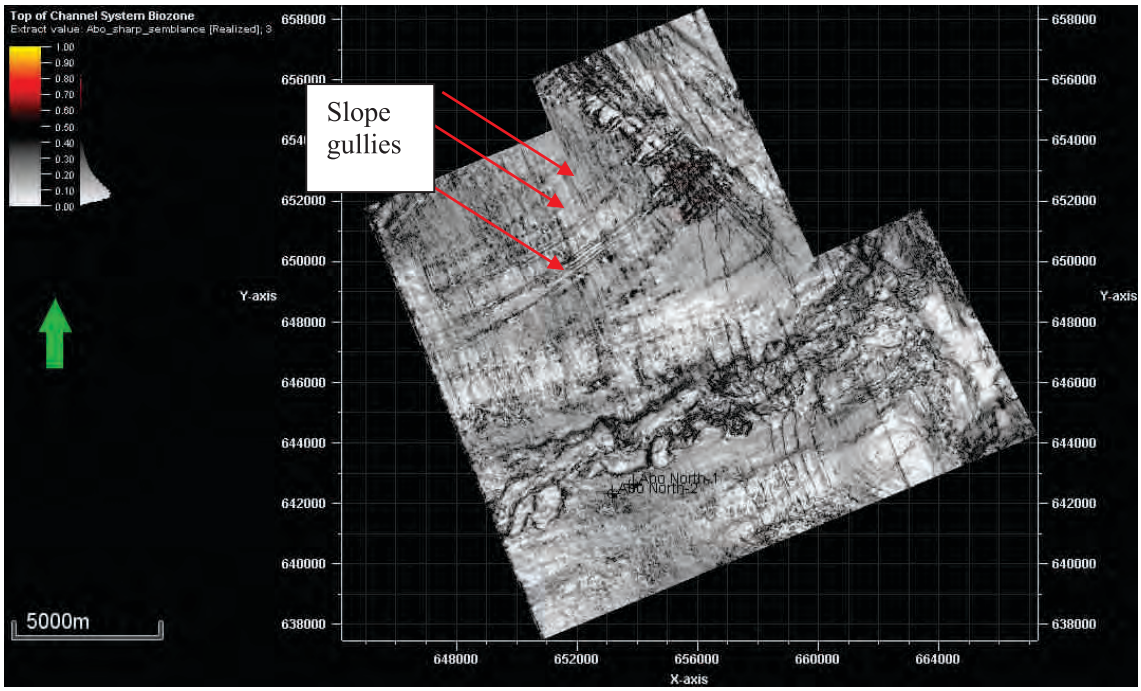


Figure 29: Semblance map of 'Top of channel system' seismic Unit. Note the northeast-southwest trending wide channel in the south with pronounced sinuosity. Also, note the straight slope gullies to the north with similar trend as the wide channel.

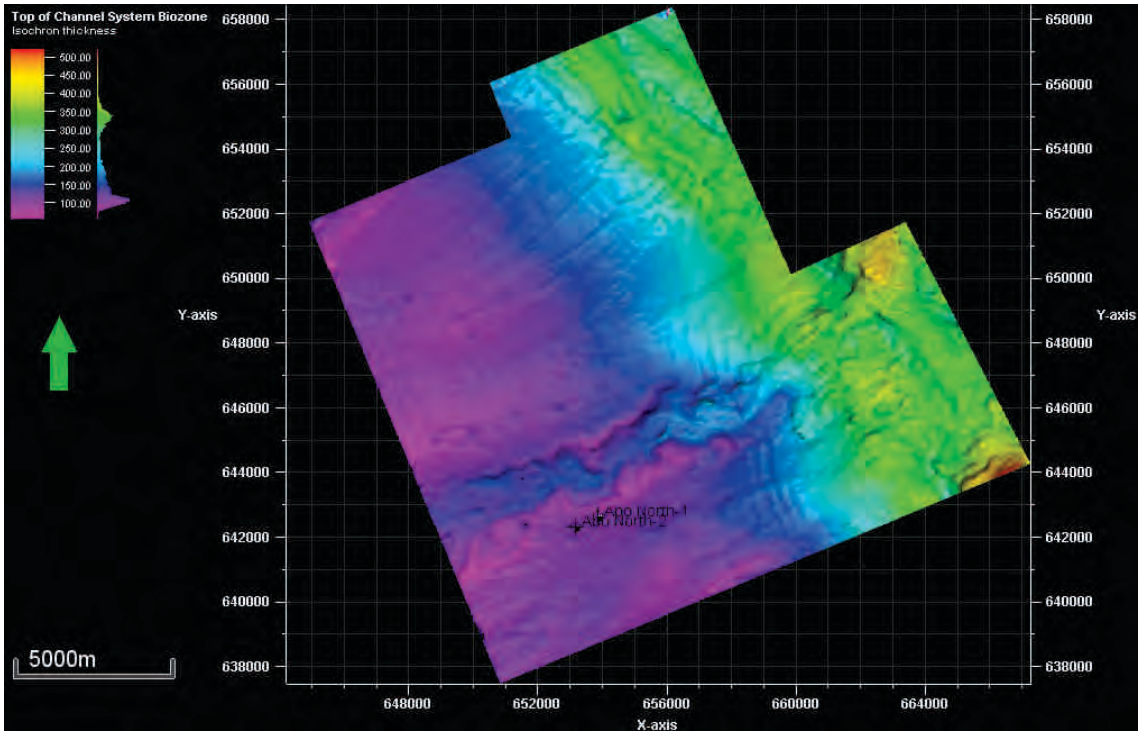


Figure 30: Thickness map of the 'Top of channel system' seismic unit. Note the occurrence of thick northeast-southwest elongated sinuous feature in the south which is thicker upslope and thins downslope and the slope gullies to the north of the seismic unit.

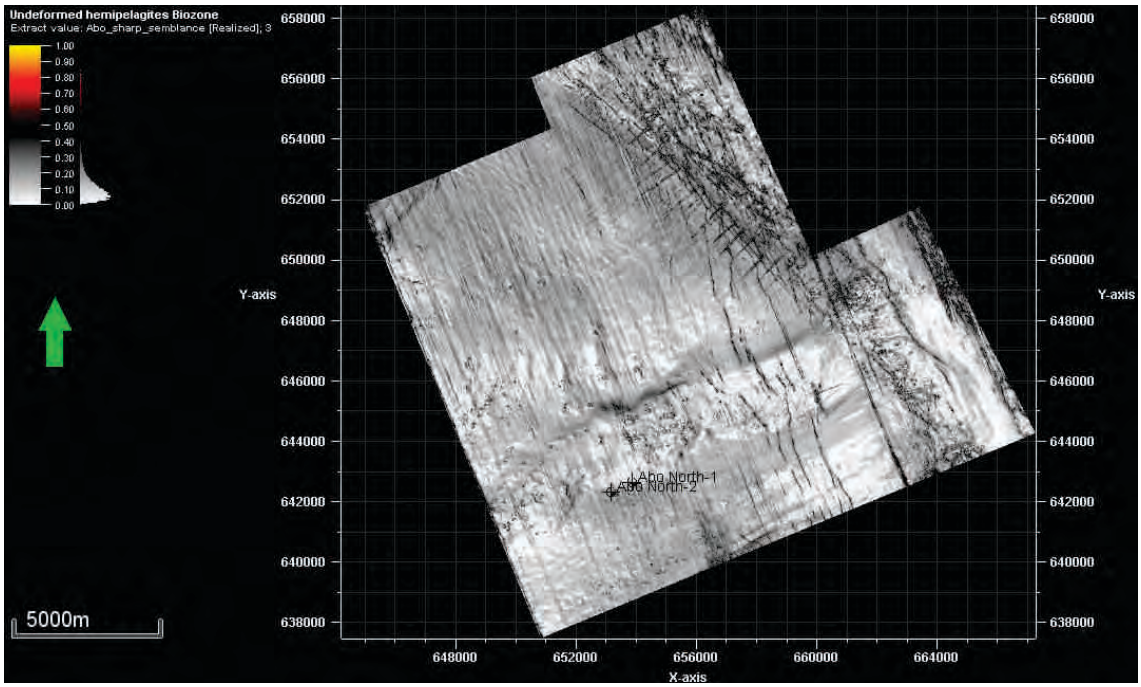


Figure 31: Semblance map of 'Undeformed hemipelagites' seismic unit. Several remnants of northeast-southwest oriented slope gullies are present in the north. Also, the area's lower half to the south shows incipient development of a precursor.

seismic facies that is interpreted as hemipelagite or marine mudstone unit.

The semblance map (Figure 23) shows a moderate semblance across the area. This is consistent with the inferred dominant spread of hemipelagites over it. The map also shows enhanced channel development with some sinuosity.

The unit's thickest part (about 300 m) occurs across the area's eastern fringes (Figure 24). Its thinnest part is about 50 m thick along a 15 km-long northeast-southwest elongated linear feature that is up to 3000 m maximum width with its flanks being up to 125 m thick. It can be considered that erosion was the dominant process within the channel with simultaneous deposition at the banks. This linear feature has implication for large transportation of sediment gravity flows downslope to the southwest.

Intra Channel-3 Seismic Unit

This base of this unit is taken as the top of the 'Intra channel 2' seismic level and its top delineated by the 'Intra channel 3' horizon (Figure 4). The internal architecture has laterally continuous high amplitude facies which can be interpreted as sandy turbidites.

The unit's semblance map (Figure 25) shows a more prominent northeast-southwest trending feature which indicated that the ancestral channel was still active with its position aligned with the underlying linear feature. Within the unit, other smaller channels (Figure 25) developed and contributed as fairway for transporting sediment gravity flows downslope.

The 'Intra Channel 3' unit is about 225 m thick in the north with a 50 m thick mound in the south (Figure 26). Its centre has a northeast-southwest trending feature (175 m and 300 m thick to the southwest and northeast respectively). Typically, its flanks are thicker than the stream, deemed the channel center. This channel axis is interpreted as depositional in nature and it denotes a receptacle or sink for sediment gravity flows.

Intra Channel-4 Seismic Unit

The 'Intra channel 4' unit has at its base as the 'Intra channel 3' seismic horizon and bounded at the top by the 'Intra channel 4' horizon. The internal facies character shows high amplitude continuous facies at the base which passes to high amplitude continuous facies with channelised chaotic core at the top (Figure 4).

The semblance map (Figure 27) largely shows similar facies across the area, but the southernmost part (denoted by a red oval line) has a different lower semblance than other areas. This lobe-like feature is consistent with the lobate feature interpreted as slope fan in Figure 28. Closer observation also shows that the lobate feature's semblance matches that of the easternmost part where the two areas are clearly linked by a feeder system (Figure 27). This denotes a complete system of likely secondary source of sediment gravity flow that is contiguous with the recipient mini basin.

The unit is thicker to the area's east reaching 300 m (Figure 28). It links to the south *via* a feeder-conduit to a lobate feature (Figure 27) with a 275 m-thick centre. To the northwest, the unit formed a 50 m-thick body and flanks a traceable 150 – 200

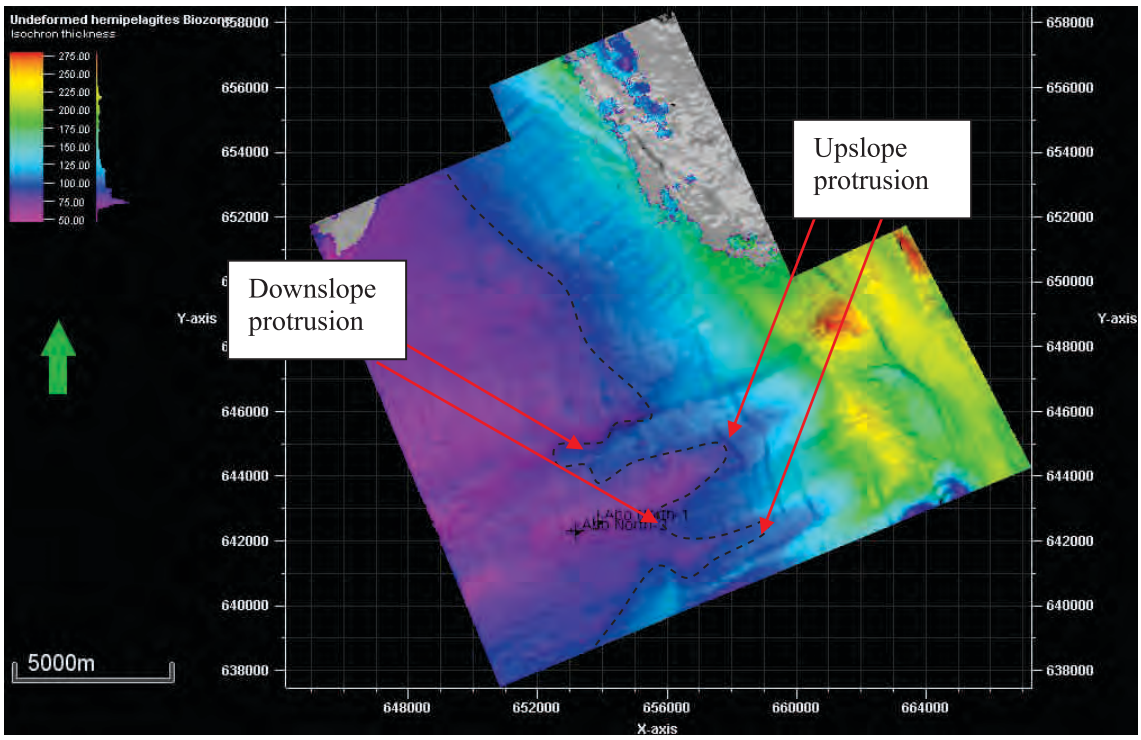


Figure 32: Thickness map of 'Undeformed hemipelagites' seismic unit. The facies generally thinned out downslope. Downslope and upslope lateral interfingering is noted in the middle of the slope.

m-thick NE-SW linear feature that can be deemed to denote the late phase of the precursor channel below the 'Intra channel 4' unit. The lobate feature at the area's southernmost tip represents a slope fan formed by the funneling of SGFs through the adjoined feeder which is connected to a staging area in the east.

Top of Channel System Seismic Unit

This unit's base is specified by 'Intra-channel 4' seismic level. Its top is bounded by the 'Top of channel' seismic horizon. Its basal facies typically has low-amplitude reflections that are interspersed by high-amplitude seismic bodies. It consists of channels with low amplitude cores (Figure 4).

This unit's semblance map shows a more advanced channelization (width > 4000 m) to the south with multiple episodes of sinuosity (Figure 29) trending northeast-southwest. In the northern part, several straight slope gullies occurred within intervals of 500 to 1000 m.

The 'Top of channel System' gradually thins westwards with a maximum thickness of 40 m and thickens to the east where the maximum is 350 m (Figure 30). At its centre is a 150 m (downslope) to 200m (upslope) thick northeast-southwest elongated sinuous feature. This east-west thickness gradation suggests that at this stage, the system is setting up for some form of slope equilibrium - where massive sediment gravity flows are trapped upslope and only fine background hemipelagic components reach the downslope milieu. The long feature with internal sinuosity denotes the unit's renewed channelization and its thicker core suggests a depositional channel (Posamentier and Walker, 2006; Straub and Mohrig, 2008; Straub and Mohrig, 2009; Straub *et al.,* 2008; Straub *et al.*, 2012).

Undeformed hemipelagites Seismic Unit

This unit's base is represented by the 'Top of channel system' seismic horizon. The unit is capped by the 'Undeformed hemipelagites' seismic horizon (Figure 4). Its internal seismic facies is typified by high amplitude laterally continuous reflections interpreted to be background sedimentation which formed into marine mudstones or hemipelagites.

The unit's semblance map (Figure 31) indicates a predominant occurrence of low semblance facies with several remnants of northeast-southwest oriented slope gullies in the north. The gullies terminate midway on the slope. Also, the area's lower half to the south shows incipient development of a channel which is about 4000 m wide.

The thickness map of the unit indicates facies thinning to about 50 m downslope. Its thicker upslope part is up to 270 m. Downslope protrusions, about 100 m thick, occur in its lower central part (Figure 32) where they laterally interfinger with their upslope counterparts. The protrusions denote the mainstreams of channels that acted as conduits for transporting sediment gravity flows from the upslope staging area.

DISCUSSION

Controls on the development and trapping of sediment gravity flows in the upper slope, offshore western Niger Delta

The integrated analysis of the available well and seismic datasets in the study area suggests that the deepwater succession is characterised by a predictable temporal and spatial stratigraphic

development (Dailly, 1983; Smith, 2004; Prather *et al.,* 1998; Pirmez *et al.,* 2000; Prather, 2000, 2020; Pyles *et al.,* 2011; Moscardelli *et al.,* 2012; Olafiranye *et al.,* 2013). The overall impact of mini-basin development from the initial tectonic diapirism at the base of the succession can be inferred. It was a key trigger for dominance of 'debrites' at this lower interval where slope instability created sediment gravity flows. Continuous flow and fill by sediment gravity flows helped to stabilize the slope and prepare the basin for lower energy turbidite system and background sedimentation. This led to temporal evolution of hemipelagites in the succession's upper part which was formed in a more quiescent depositional setting.

Evolution of accommodation and topographic partitioning of the biostratigraphically constrained units in the upper slope environment

Slope mini basins arose all over the lower part of the study area. The basal *Ammobaculites agglutinans* marker surface map (Figure 6) is an example. They are believed to have been formed in response to diapirism undergone by the deep-seated marine substrates of the underlying Akata Formation consistent with Kulke (1995) and Damuth (1994). These interpreted mini basins correspond to ponded accommodation and the associated topographic splitting that have also been identified by Mutti and Normark, (1987), Bouma (2004), Prather *et al. (*1998), Booth *et al. (*2000), and Prather (2020). This was so during the deposition of the biostratigraphically constrained units from the *Globorotalia merotumida* to the *Globorotalia margaritae* surfaces. The basal *Globorotalia merotumida* unit's thickest part indicates a 500m maximum topographic relief created then. Layered, sheet-like sandstones often typify ponded accommodation fill with a mini-basin shape that ruled the palaeoslope (e.g., Olafiranye, *et al*. (2013). The overlying *Globoquadrina dehiscens, Globigerina tumida, Globigerina nepenthes* and *Globorotalia merotumida* units show similar topographic patterns. Aside their ponded accommodation, NE-SW-trending embryonic channelisation arose and increasingly matured in the middle of the *Globoquadrina dehiscens, Globigerina tumida, Globigerina nepenthes,* and *Globorotalia merotumida* units. This tallies with slope milieu degrading to form 'above grade' profile which give rise to pinchout of sands or stratigraphic onlap within the mini basins to form stratigraphic traps with propensity hydrocarbon accumulation.

Evolution of accommodation and topographic healing created by the biostratigraphically unconstrained units in the upper slope environment

The development of slope gullies and canyons in the Intra Channel-1, -2, -3, -4, and the Top Channel System seismic units enabled sediment gravity flows to bypass the upslope setting and get transferred downslope into the deeper water. Prather (2000, 2020) demonstrated this process and effect in studies using data in the Gulf of Mexico (GoM), offshore Venezuela, Campos Basn, Lower Congo slope, the Niger Delta, North Sea, NW Borneo, Tarakan Basin and Mahakam Delta and discovered that high concentration of sediment gravity flows occurs across mid-slope and toe-of-slope regions in a variety of accommodation types including ponded, healed-slope, and incised submarine valley. Channel

development is distinct during evolution of the 'Intra channel 1' time and advanced during the 'Intra channel 2' event. However, evolution of the 'Intra channel 3' units healed the precursor channel with attendant sediment gravity flows infill similar to that observed by Beaubouef and Friedmann (2000), and Steffens *et al.* (2003). It is deduced that the channel-imprinted biostratigraphically unconstrained interval units (Intra Channel-1, Intra channel-2, Intra channel-3, and Intra channel-4) underwent aggradation as the slope depositional system internally re-adjusted to attain equilibrium profile and be at grade. Afterwards, the depositional profile rapidly returned to a slope degradation and sediment bypass phase via re-initiation of the channel geometry in when Intra channel- 4 began to emerge. At this time, some slope gullies created in the north acted as secondary conduits, funneling sediments to the downslope milieu. The system then healed again while the 'Top channel system' and 'Undeformed hemipelagites' units deposited.

The fluctuating slope accommodation resulted from a constructive (aggradational-progradational) and destructive (degradational) interplay of a slope system that dynamically achieved an equilibrium profile. This was a sum of grade and above-grade profiles analogous to Haughton (1994), Prather *et al*. (1998), Kneller and McCaffrey (1999), Prather (2000, 2020), Bouma (2004), Hodgson and Haughton (2004), Smith (2004), Adeogba *et al*. (2005), Hodgson *et al*. (2011), Moscardelli *et al*. (2012), Olafiranye *et al*. (2013), Prather, 2020; Casagrande *et al*. (2024).

CONCLUSION

This study pooled high resolution biostratigraphic, and good quality 3D seismic data, over a 300 km^2 offshore western Niger Delta area. Its major conclusions are as follows:

1. Based on the vertical biostratigraphic data coverage, the entire sequence can be subdivided into two (2) broad intervals: a lower biostratigraphically-constrained part and an upper unconstrained section. These are further divisible into five (5) and six (6) stratigraphic units respectively. Analysis of each unit's debritic, turbiditic and hemipelagic seismic facies tied them to depositional regime and products.
2. Seismic interpretation revealed incidence of mini-basins and inter-basin topographic divides. This resulted from diapirism suffered by the deep-seated underlying marine shales below the study section's lower biostratigraphically-constrained interval. The existence of the mini basins led to the widespread evolution of ponded accommodation.
3. The basins' varied topographic relief, with a maximum of 900 m, across the stratigraphic surfaces influenced the distribution of sediments with differing thicknesses.
4. Progressive healing of the mini-basins made the system more channel-prone. This gave a slope profile apt for creating a system that fostered efficient sediment bypass where flushing, transfer, and delivery took sediment downslope.
5. Progressive channelization was later curbed by healing capacity of background hemipelagic drapes. That aided the profile to attain grade with the inherent trait of slope profiles to ultimately attain

equilibrium.

6. The stratigraphic units are so predictably set up that the bottom diapirically-initiated mini-basins are typified by debris flows. This unit underlies a waning energy turbidite system plus background deposition of hemipelagites in the upper part of the succession.
7. The biostratigraphically-constrained aspects of the results provide extended relationship for predicting the deep-seated topographic structuration as well as depositional processes and products associated with sediment gravity flows in adjoining areas of the study.

REFERENCES

Adegoke, O. S., Oyebamiji, A. S., Edet, J. J., Osterloff, P. L., Ulu,O. K. (Eds) (2017). Cenozoic foraminifera and calcareous nanno-fossil biostratigraphy of the Niger Delta. Amsterdam, Netherlands, Elsevier, 592p.

Adeogba, A. A., McHargue, T. R., Graham, S. A., 2005. Transient fan architecture and depositional controls from near-surface 3-D seismic data, Niger Delta continental slope. *AAPG Bulletin,* vol. 89 (5), p. 627-643.

Alves, T. M., 2010. **3D Seismic examples of differential compaction in mass-transport deposits and their effect on post-failure strata**. *Marine Geology*, vol. 271, p. 212-224.

Armitage, D. A., Romans, B. W., Covault, J. A., Graham, S. A., 2009. The influence of mass-transport-deposit surface topography on the evolution of turbidite architecture: The Sierra Contreras, Tres Pasos Formation (Cretaceous), southern Chile. *Journal of Sedimentary Research* vol. 79, pp. 287–301.

Armitage, D. A., Stright, L., 2010. Modelling and interpreting the seismic-reflection expression of sandstone in an ancient mass-transport deposit dominated deep-water slope environment. *Marine and Petroleum Geology*, vol. 27, p. 1-12.

Bauer, D. B., Hubbard, S. M., Covault, J. A., & Romans, B. W. (2020). Inherited depositional topography control on shelf-margin oversteepening, readjustment, and coarse-grained sediment delivery to deep water, Magallanes Basin, Chile. *Frontiers in Earth Science*, vol. 7, 358p.

Beaubouef, R. T., Friedman, S. J. 2000. High resolution seismic/sequence stratigraphic framework for the evolution of Pleistocene intra-slope basins, Western Gulf of Mexico: depositional models and reservoir analogues. *In:* WEIMER, P., SLATT, *R. M. et al.* (eds) *Deep-Water Reservoirs of the World.* Proceedings Gulf Coast Section Society of Economic Palaeontologists and Mineralogists Foundation 20th Annual Bob F. Perkins Research Conference, CD-ROM.60.

Haughton, P. D. (1994). Deposits of deflected and ponded turbidity currents, Sorbas Basin, Southeast Spain. Journal of sedimentary Research, 64(2a), 233-246.

Bilotti, F and Shaw, J. H., 2005. Deep-water Niger Delta fold and thrust belt modeled as a critical-taper wedge: the influence of elevated basal fluid pressure on structural styles Am. Assoc. *Pet. Geol. Bull.*, vol. 89,

p. 1475-1491.

Booth, J. R., DuVernay III, A. E., Pfeiffer, D. S., and Styzen, M. J., 2000. Sequence stratigraphic framework, depositional models, and stacking patterns of ponded and slope fan systems in the Auger Basin: Central Gulf of Mexico slope In: Weimer, P., Slatt, R. M., Coleman, J.. Rossen, N. C., Nelson, H., Bouma, A. H., Styzen, M. J. and Lawrence, D. T. (eds.), Deep-water reservoirs of the world: Gulf Coast Section. *SEPM 20th Annual Perkins Research Conference,* pp. 82– 103.

Bouma, A. H. (2004). Key controls on the characteristics of turbidite systems. *Geological Society, London*, Special Publications, vol. 222(1), p. 9-22.

Casagrande, J., Hodgson, D. M., & Peakall, J. (2024). A salty snapshot: extreme variations in basal erosion patterns preserved in a submarine channel. *Journal of the Geological Society, vol. 181(2,) p. 1-11.*

Catuneanu, O., Galloway, W. E., Kendall, C. G. St. C., Miall, A. D., Posamentier, H. W., Strasser, A., Tucker, M. E., 2011. **Sequence stratigraphy: methodology and nomenclature.** *Newsletters on Stratigraphy*, vol. 44 (3) , p. 173-245.

Corredor, F., Shaw, J. H. and Bilotti, F., 2005, Structural styles in the deepwater fold-and-thrust belts of the Niger Delta: *AAPG Bulletin*, v. 89, no. 6, pp. 753– 780.

Dailly, G. C., 1983. Slope readjustment during sedimentation of continental margins. In: Watkins, J. S., Drake, C. L. (eds.), Studies in Continental Marine Geology. *American Association of Petroleum Geologists Memoirs* vol. 34, p. 593-608.

Damuth, J. E., 1994. Neogene gravity tectonics and depositional processes on the deep Niger Delta continental margin *Mar. Pet. Geol.*, vol. 11 (3), p. 320-346.

Daniels, B. G., Hubbard, S. M., Stright, L., Romans, B. W. (2024). Downslope variability in deep-water slope channel fill facies and stacking patterns. *Marine and Petroleum Geology*, vol. 165, p. 1-25.

Doust, H. and Omatsola, M. E. (1990). Niger Delta. In: Edwards, J. D., Santogrossi, P. A. (eds.), Divergent Passive Margin Basins, *A.A.P.G. Memoir* vol. 48, p. 201 - 238.

Evamy, B.D., Haremboure, J., Kamerling, P., Knaap, W.A., Molloy, F.A., Rowlands, P.H., 1978. Hydrocarbon habitat of Tertiary Niger delta. *AAPG Bull.* Vol. 62, p. 1–39.

Galloway W. E., 1989. Genetic stratigraphic sequences in basin analysis, I. Architecture and genesis of flooding-surface bounded depositional units, *American Association of Petroleum Geologists Bulletin* vol. 73, p. 125–142.

Hodgson, D. M. and Haughton, P. D. W., (2004). Impact of Syn-depositional Faulting on Gravity Current Behaviour and Deep-water Stratigraphy: Tabernas-Sorbas Basin, SE Spain. In: *Geological Society, London, Special Publications*, vol. 222(1), p. 135-158.

Hodgson, D., Di Celma, C., Brunt, R., Flint, S.S., (2011). Submarine slope degradation and aggradation and the stratigraphic evolution of channel-levee systems. *J. Geol. Soc. Lond.* Vol. 168, p. 625-628.

Haughton, P. D. (1994). Deposits of deflected and ponded turbidity currents, Sorbas Basin, Southeast Spain. *Journal of sedimentary Research*, vol. 64(2a), p. 233-246.

Jackson, C. A. L. and Johnson, H. D., 2009. Sustained turbidity currents and their interaction with debrite-related topography: Labuan Island, offshore NW Borneo, Malaysia. *Sedimentary Geology*, vol. 219(1-4), p. 77-96.

Jackson, C. A. L., Zakaria, A. A., Johnson, H. D., Tongkul, F.and Crevello, P. D., 2009. Sedimentology, stratigraphic occurrence and origin of linked debrites in the West Crocker Fm (Oligo-Miocene), Sabah, NW Borneo. *Marine and Petroleum Geology*, vol. 26(10), p. 1957-1973.

Kneller, B., and McCaffrey, W. B., 1999. Depositional effects of flow non-uniformity and stratification within turbidity currents approaching a bounding slope: deflection, reflection and facies variations. *Journal of Sedimentary Research* vol. 69, p. 980-991.

Kulke, H., (1995). Nigeria, in, Kulke, H., ed., Regional Petroleum Geology of the World. Part II: Africa, America, Australia and Antarctica: *Berlin, Gebrüder Borntraeger*, pp. 143-172.

Lehner, P., and De Ruiter, P.A.C., 1977, Structural history of Atlantic Margin of Africa: *American Association of Petroleum Geologists Bulletin*, vol. 61, p. 961-981.

Macdonald, H. A., Peakall, J. and Wignall, P. B., 2011. Thickening-upward sequences Sedimentation in deep-sea lobe-elements: implications for the origin of thickening-upward sequences. Journal of the Geological Society vol. 168; p. 319-332. doi: 10.1144/0016-76492010-036.

McHargue, T., 1991. Seismic facies, processes, and evolution of Miocene inner fan channels, Indus Submarine Fan. In: Weimer, P., Link, M. (Eds.), Seismic Facies and Sedimentary Processes of Submarine Fans and Turbidite Systems. *Springer-Verlag, New York*, 402-413p.

Moscardelli, L., Wood, L. J., Dunlap, D. B., 2012. Shelf-edge deltas along structurally complex margins: a case study from eastern offshore Trinidad. *AAPG Bulletin* vol. 96 (8), p. 1483-1522.

Mutti, E. (1985) Turbidite systems and their relations to depositional sequences. In: Provenance of Arenites (Ed. By G. G. Zuffa),. *Reidel Publishing Company, Dortrecht*. P. 65-93

Mutti, E., Normark, W. R., 1987. Comparing examples of modern and ancient turbidite systems: problems and concepts. In: Legget, J. K., Zuffa, G. G. (Eds.), Marine Clastic Sedimentology. *Graham and Trotman, London*, p. 1-38.

Olafiranye, K., Jackson, C. A. L. and Hodgson, D. M., 2013. The role of tectonics and mass-transport complex emplacement on upper slope stratigraphic evolution: A 3D seismic case study from offshore Angola. *Marine and Petroleum Geology*, vol. 44, 2013, p. 196-216.

Omosanya, K. O., & Alves, T. M. (2013). A 3-dimensional seismic method to assess the provenance of Mass-Transport Deposits (MTDs) on salt-rich continental slopes (Espírito Santo Basin, SE Brazil). *Marine and Petroleum Geology*, vol. 44, p. 223-

239.

Pirmez, C., Beaubouef, R.T., Friedmann, S.J., Mohrig, D.C. (2000). Equilibrium profile and base level in submarine channels: examples from Late Pleistocene systems and implications for the architecture of deep-water reservoirs, in Weimer, P., Slatt, R.M., Coleman, J., Rosen, N.C., Nelson, H., Bouma, A.H., Styzen, M.J., and Lawrence, D.T., eds., Deep-Water Reservoirs of the World: Gulf Coast Society of the Society of Economic Paleontologists and Mineralogists Foundation, 20th Annual Research Conference, p. 782–805. 2000, Houston, TX.

Posamentier, H. W., and Kolla, V., 2003. Seismic geomorphology and stratigraphy of depositional elements in deep-water settings. *Journal of Sedimentary Research* vol. 73, 3, p. 367–388.

Posamentier, H. W. and Walker, R. G., 2006. Deep-water turbidites and submarine fans. In: Posamentier, H. W., Walker, R. G. (eds.), Facies Models Revisited. *Society for Sedimentary Geology (SEPM), Special Publication,* vol. 84, p. 397–520.

Prather, B. E., 2000. Calibration and visualization of depositional process models for above-grade slopes: a case study from the Gulf of Mexico. *Marine and Petroleum Geology* vol. 17, p. 619-638.

Prather, B. E. (2020). Controls on reservoir distribution, architecture and stratigraphic trapping in slope settings. In *Regional Geology and Tectonics, Elsevier*, p. 481-515.

Prather, B. E., Booth, J. R., Steffens, G. S., and Craig, P. A., 1998. Classification, lithologic calibration, and stratigraphic succession of seismic facies of intraslope basins, deep-water Gulf of Mexico. *AAPG Bulletin,* vol. 82, p. 701–728.

Pyles, D. R., Syvitski, J. P. M., Slatt, R. M., 2011. Defining the concept of stratigraphic grade and applying it to stratal (reservoir) architecture and evolution of the slope-to-basin profile: an outcrop perspective. *Marine and Petroleum Geology,* vol. 28, p. 675-697.

Rebesco, M., Stow, D. A. V., 2001. **Seismic expression of contourites and related deposits: a preface.** *Marine Geophysical Research*, vol. 22, p. 303-308.

Sawyer, D. E, Flemings, P. B. and Shipp, R. C., 2007. **Seismic geomorphology, lithology, and evolution of the late Pleistocene Mars-Ursa turbidite region, Mississippi Canyon area, northern Gulf of Mexico,** *American Association of Petroleum Geology Bulletin*, vol. 91, p. 215-234.

Short, K. C. and Stauble, A. J., (1967). Outline of Geology of Niger Delta. *Amer. Assoc. Petrol. Geol. Bull.* Vol. 51(5): p. 761-779.

Smith, R. D. A., 2004. Silled sub-basins to connected tortuous corridors: sediment distribution systems on topographically complex sub-aqueous slopes. In: Lomas, S. A. and Joseph, P. (Eds.), Confined Turbidite Systems. *Geological Society London Special Publications*, vol. 222, p. 23-43.

Sprague, A., Garfield, T., Goulding, F., Beaubouef, R., Sullivan, M., Rossen, C., Campion, K., Sickafoose, D., Abreu, D.,

Schellpeper, M., Jensen, G., Jennette, D., Pirmez, C., Dixon, B., Ying, D., Ardill, J., Mohrig, D., Porter, M., Farrell, M., Mellere, D., 2005. Integrated slope channel depositional models: the key to successful prediction of reservoir presence and quality in offshore West Africa, CIPM, cuarto E-Exitep. Veracruz, Mexico, pp. 1-13.

Steffens, G. S., Biegert, E. K., Scott Sumner, H. and Bird, D., 2003. Quantitative bathymetric analyses of selected deepwater siliciclastic margins: receiving basin configurations for deepwater fan systems, *Marine and Petroleum Geology*, vol. 20(6-8), p. 547-561.

Straub, K. M. and Mohrig, D., 2008. Quantifying the morphology and growth of levees in aggrading submarine channels: Journal of Geophysical Research, vol. 113, p. 1-20. Paper F03012,

Straub, K. M. and Mohrig, D., 2009. Constructional canyons built by sheet-like turbidity currents: observations from offshore Brunei Darussalam: *Journal of Sedimentary Research,* vol. 79, p. 24–39.

Straub, K. M., Mohrig, D., McElroy, B., Buttles, J. and Pirmez, C., 2008. Interactions between turbidity currents and topography in aggrading sinuous submarine channels: A laboratory study: *Geological Society of America, Bulletin*, vol. 120, p. 368–385.

Straub, K. M., Mohrig, D. and Pirmez, C., 2012. Architecture of an aggradational tributary submarine-channel network on the continental slope, offshore Brunei Darussalam, in Case Studies from Seafloor and Near Seafloor Analogues: *Tulsa, SEPM (Society for Sedimentary Geology) Special Publication* vol. 99, p. 13–30.

Tian, R., Xian, B., Wu, Q., Shu, Q., Liu, J., Zhang, W., Wang, J. (2023). Turbidite system controlled by fault interaction and linkage on a slope belt of rift basin: Zhanhua depression, Bohai Bay Basin, China. *Marine and Petroleum Geology*, vol. 155, p. 1-18.

Tuttle, M. L., Charpentier, R. R., & Brownfield, M. E. (1999). The Niger Delta Petroleum System: Niger Delta Province, Nigeria, Cameroon, and Equatorial Guinea, Africa US Department of the Interior, *US Geological Survey*. (pp. 99-50).

Van der Merwe, W. C., Flint, S. S. and Hodgson, D. M., 2010. Sequence stratigraphy of an argillaceous, deepwater basin-plain succession: Vischkuil Formation (Permian), Karoo Basin, South Africa. *Marine and Petroleum Geology,* vol. 27, p. 321–333.

Walker, R. G. (1967). Turbidite sedimentary structures and their relationship to proximal and distal depositional environments. *Journal of Sedimentary Research*, vol. 37(1), p. 25-43.

Weimer, P. and Slatt, R. M., 2007. Petroleum geology of deepwater settings. *AAPG Studies in Geology*, vol. 57, 816p.

Xiao, H. and Suppe, J. (1992). Origin of Rollover, *AAPG Bulletin*, vol, 76, p. 509-529.